

1 **Holocene climate aridification trend and human impact interrupted by millennial- and**
2 **centennial-scale climate fluctuations from a new sedimentary record from Padul (Sierra**
3 **Nevada, southern Iberian Peninsula)**

4 María J. Ramos-Román¹, Gonzalo Jiménez-Moreno¹, Jon Camuera¹, Antonio García-Alix¹,
5 R. Scott Anderson², Francisco J. Jiménez-Espejo³, José S. Carrión⁴

6 ¹ Departamento de Estratigrafía y Paleontología, Universidad de Granada, Spain

7 ² School of Earth Sciences and Environmental Sustainability, Northern Arizona University,
8 USA.

9 ³ Department of Biogeochemistry, Japan Agency for Marine-Earth Science and Technology
10 (JAMSTEC), Japan.

11 ⁴ Departamento de Biología Vegetal, Facultad de Biología, Universidad de Murcia, Murcia,
12 Spain.

13 *Correspondence to:* María J. Ramos-Román (mjrr@ugr.es)

14 **Abstract.** Holocene centennial-scale paleoenvironmental variability has been described in a
15 multiproxy analysis (i.e. lithology, geochemistry, macrofossil and microfossil analyses) of a
16 paleoecological record from the Padul basin in Sierra Nevada, southern Iberian Peninsula.
17 This sequence covers a relevant time interval hitherto unreported in the studies of the Padul
18 sedimentary sequence. The ~4700 yr-long record has preserved proxies of climate variability,
19 with vegetation, lake levels and sedimentological change during the Holocene in one of the
20 most unique and southernmost wetland from Europe. The progressive Middle and Late
21 Holocene trend toward arid conditions identified by numerous authors in the western
22 Mediterranean region, mostly related to a decrease in summer insolation, is also documented
23 in this record, being here also superimposed by centennial-scale variability in humidity. In
24 turn, this record shows centennial-scale climate oscillations in temperature that correlate with
25 well-known climatic events during the Late Holocene in the western Mediterranean region,
26 synchronous with variability in solar and atmospheric dynamics. The multiproxy Padul
27 record first shows a transition from a relatively humid Middle Holocene in the western
28 Mediterranean region to more aridity from ~4700 to ~2800 cal yr BP. A relatively warm and
29 humid period occurred between ~2600 to ~1600 cal yr BP, coinciding with persistent
30 negative NAO conditions and the historic Iberian-Roman Humid Period. Enhanced arid
31 conditions, co-occurring with overall positive NAO conditions and increasing solar activity,
32 are observed between ~1550 to ~450 cal yr BP (~400 to ~1400 CE) and colder and warmer
33 conditions happened during the Dark Ages and Medieval Climate Anomaly, respectively.
34 Slightly wetter conditions took place during the end of the MCA and the first part of the
35 Little Ice Age, which could be related to a change towards negative NAO conditions and
36 minima in solar activity. Time series analysis performed from local (*Botryococcus* and TOC)
37 and regional (Mediterranean forest) signals helped us determining the relationship between
38 southern Iberian climate evolution, atmospheric, oceanic dynamics and solar activity. Our
39 multiproxy record shows little evidence of human impact in the area until ~1550 cal yr BP,
40 when evidence of agriculture and livestock grazing occurs. Therefore climate is the main
41 forcing mechanism controlling environmental change in the area until relatively recently.

42

43 **Keywords:** Holocene, Padul, peat bog, North Atlantic Oscillation, atmospheric dynamics,
44 southern Iberian Peninsula, Sierra Nevada, western Mediterranean.

45 1 Introduction

46 The Mediterranean area is situated in a sensitive region between temperate and subtropical
47 climates making it an important place to study the connections between atmospheric and
48 oceanic dynamics and environmental change. Climate in the western Mediterranean and the
49 southern Iberian Peninsula is influenced by several atmospheric and oceanic dynamics
50 (Alpert et al., 2006), including the North Atlantic Oscillation (NAO) one of the principal
51 atmospheric phenomenon controlling climate in the area (Hurrell, 1995; Moreno et al., 2005).
52 Recent NAO reconstructions in the western Mediterranean relate negative and positive NAO
53 conditions with an increase and decrease, respectively, in winter (effective) precipitation
54 (Olsen et al., 2012; Trouet et al., 2009). Numerous paleoenvironmental studies in the western
55 Mediterranean have detected a link at millennial- and centennial-scales between the
56 oscillations of paleoclimate proxies from sedimentary records with solar variability and
57 atmospheric (i.e., NAO) and/or ocean dynamics during the Holocene (Fletcher et al., 2013;
58 Moreno et al., 2012; Rodrigo-Gámiz et al., 2014). Very few montane and low altitude lake
59 records in southern Iberia document centennial-scale climate change [see, for example Zoñar
60 Lake (Martín-Puertas et al., 2008)], with most terrestrial records in the western
61 Mediterranean region evidencing only millennial-scale cyclical changes. Therefore, higher-
62 resolution decadal-scale analyses are necessary to analyze the link between solar activity,
63 atmospheric and oceanographic systems with terrestrial environment in this area at shorter
64 (i.e., centennial) time scales.

66 Sediments from lakes, peat bogs and marine records from the western Mediterranean have
67 documented an aridification trend during the Late Holocene (Carrión et al., 2010; Gil-
68 Romera et al., 2010; Jalut et al., 2009). This trend, however, was superimposed by shorter-
69 term climate variability, as shown by several recent studies from the region (Carrión, 2002;
70 Fletcher et al., 2013; Jiménez-Moreno et al., 2013; Martín-Puertas et al., 2008; Ramos-
71 Román et al., 2016). This relationship between climate variability, culture evolution and
72 human impact during the Late Holocene has also been the subject of recent
73 paleoenvironmental studies (Carrión et al., 2007; Lillios et al., 2016; López-Sáez et al., 2014;
74 Magny, 2004). However, it is still unclear whether climate or human activities have been the
75 main forcing driving environmental change (i.e., deforestation) in this area during this time.

77 Within the western Mediterranean, Sierra Nevada is the highest and southernmost mountain
78 range in the Iberian Peninsula and thus presents a critical area for paleoenvironmental
79 studies. Most high-resolution studies there have come from high elevation sites. The well-
80 known Padul wetland site is located at the western foot of the Sierra Nevada (Fig. 1) and
81 bears one of the longest continental records in southern Europe, with a sedimentary sequence
82 of ~100 m thick that could represent the last 1 Ma (Ortiz et al., 2004). Several research
83 studies, including radiocarbon dating, geochemistry and pollen analyses, have been carried
84 out on previous cores from Padul, and have documented glacial/interglacial cycles during the
85 Pleistocene and up until the Middle Holocene. However, the Late Holocene section of the
86 Padul sedimentary sequence has never been effectively retrieved and studied (Florschütz et
87 al., 1971; Ortiz et al., 2004; Pons and Reille, 1988). This was due to the location of these
88 previous corings within a current peat mine operation, where the upper (and non-productive)
89 part of the sedimentary sequence was missing.

91 Here we present a new record from the Padul basin: Padul-15-05, a 42.64 m-long sediment
92 core that, for the first time, contains a continuous record of the Late Holocene (Fig. 2). A
93 high-resolution multi-proxy analysis of the upper 1.15 m, the past ~4700 cal yr BP, has

94 allowed us to determine a complete paleoenvironmental and paleoclimatic record at
95 centennial- and millennial-scales. To accomplish that, we reconstructed changes in the Padul
96 vegetation, sedimentation, climate and human impact during the Holocene throughout the
97 interpretation of the lithology, palynology and geochemistry.

98

99 Specifically, the main objective of this paper is to determine environmental variability and
100 climate evolution in the southern Iberian Peninsula and the western Mediterranean region and
101 their linkages to northern hemisphere climate and solar variability during the latter Holocene.
102 In order to do this, we compared our results with other paleoclimate records from the region
103 and solar activity from the northern hemisphere for the past ~4700 cal yr BP (Bond et al.,
104 2001; Laskar et al., 2004; Sicre et al., 2016; Steinhilber et al., 2009).

105 **2 Regional setting: Padul, climate and vegetation**

106 Padul is located at the foothill of Sierra Nevada, which is a W-E aligned mountain range
107 located in Andalucía (southern Spain; Fig. 1). Climate in this area is Mediterranean, with cool
108 and humid winters and hot/warm summer drought. Sierra Nevada is strongly influenced by
109 thermal and precipitation variations due to the altitudinal gradient (from ca. 700 to more than
110 3400 m), which control plant taxa distribution in different bioclimatic vegetation belts due to
111 the variability in thermotypes and ombrotypes (Valle Tendero, 2004). According to the
112 climatophilous series classification, Sierra Nevada is divided in four different vegetation belts
113 (Fig. 1). The crioromediterranean vegetation belt, occurring above ~2800 m, is characterized
114 by tundra vegetation and principally composed by species of Poaceae, Asteraceae,
115 Brassicaceae, Gentianaceae, Scrophulariaceae and Plantaginaceae between other herbs, with
116 a number of endemic plants (e.g. *Erigeron frigidus*, *Saxifraga nevadensis*, *Viola crassiuscula*,
117 *Plantago nivalis*). The oromediterranean belt, between ~1900 to ~2800 m, is principally
118 made up of *Pinus sylvestris*, *P. nigra* and *Juniperus* spp. and other shrubs such as species of
119 Fabaceae, Cistaceae and Brassicaceae. The supramediterranean belt, from ~1400 to 1900 m
120 of elevation, bears principally *Quercus pyrenaica*, *Q. faginea* and *Q. rotundifolia* and *Acer*
121 *opalus* ssp. *granatense* with other trees and shrubs, including members of the Fabaceae,
122 Thymelaeaceae, Cistaceae and *Artemisia* sp. being the most important. The
123 mesomediterranean vegetation belt occurs between ~600 and 1400 m of elevation and is
124 principally characterized by *Quercus rotundifolia*, some shrubs, herbs and plants as *Juniperus*
125 sp., and some species of Fabaceae, Cistaceae and Liliaceae with others (El Aallali et al.,
126 1998; Valle, 2003). The human impact over this area, especially important during the last
127 millennium, affected the natural vegetation distribution through fire, deforestation,
128 cultivation (i.e., *Olea*) and subsequent reforestation (mostly *Pinus*) (Anderson et al., 2011).
129 The Padul basin is situated in the mesomediterranean vegetation belt at approximately 725 m
130 elevation in the southeastern part of the Granada Basin. In this area and besides the
131 characteristic vegetation at this elevation, nitrophilous communities occur in soils disrupted
132 by livestock, pathways or open forest, normally related with anthropization (Valle, 2003).
133 This is one of the most seismically active areas in the southern Iberian Peninsula with
134 numerous faults in NW-SE direction, with the Padul fault being one of these active normal
135 faults (Alfaro et al., 2001). It is a small extensional basin approximately 12 km long and
136 covering an area of approximately 45 km², which is bounded by the Padul normal fault. The
137 sedimentary in-filling of the basin consists of Neogene and Quaternary deposits; Upper
138 Miocene conglomerates, calcarenites and marls, and Pliocene and Quaternary alluvial
139 sediments, lacustrine and peat bog deposits (Sanz de Galdeano et al., 1998; Delgado et al.,
140 2002; Domingo et al., 1983).

141
142 The Padul wetland is endorheic, with a surface of approximately 4 km² placed in the Padul
143 basin that contains a sedimentary sequence characterized mostly by peat accumulation. The
144 basin fill is asymmetric, with thicker sedimentary and peat infill to the northeast (~100 m
145 thick; Domingo-García et al., 1983; Florschütz et al., 1971; Nestares and Torres, 1997) and
146 progressively becoming thinner to the southwest (Alfaro et al., 2001). The main source area
147 of allochthonous sediments in the bog is the Sierra Nevada, which is characterized at higher
148 elevations by Paleozoic siliceous metamorphic rocks (mostly mica-schists and quartzites)
149 from the Nevado-Filabride complex and, at lower elevations and acting as bedrock, by
150 Triassic dolomites, limestones and phyllites from the Alpujarride Complex (Sanz de
151 Galdeano et al. 1998). Geochemistry in the Padul sediments is influenced by detritic
152 materials also primarily from from the the Sierra Nevada (Ortiz et al., 2004). Groundwater
153 inputs into the Padul basin come from the Triassic carbonates aquifers (N and S edge to the
154 basin), the out flow of the Granada Basin (W edge to the basin) and the conglomerate aquifer
155 to the east edge (Castillo Martín et al., 1984; Ortiz et al., 2004). The main water output is by
156 evaporation and evapotranspiration, water wells and by canals (“madres”) that drain the water
157 to the Dúrcal river to the southeast (Castillo Martín et al., 1984). Climate in the Padul area is
158 characterized by a mean annual temperature of 14.4 °C and a mean annual precipitation of
159 445 mm (<http://www.aemet.es/>).

160 The Padul-15-05 drilling site was located ~50 m south of the present-day Padul lake shore
161 area. This basin area is presently subjected to seasonal water level fluctuations and is
162 principally dominated by *Phragmites australis* (Poaceae). The lake environment is dominated
163 by aquatic and wetland communities with *Chara vulgaris*, *Myriophyllum spicatum*,
164 *Potamogeton pectinatus*, *Potamogetum coloratus*, *Phragmites australis*, *Typha*
165 *dominguensis*, *Apium nodiflorum*, *Juncus subnodulosus*, *J. bufonius*, *Carex hispida* and
166 *Ranunculus muricatus*, among others (Pérez Raya and López Nieto, 1991). Some sparse
167 riparian trees occur in the northern lake shore, such as *Populus alba*, *Populus nigra*, *Salix* sp.,
168 *Ulmus minor* and *Tamarix*. At present *Phragmites australis* is the most abundant plant
169 bordering the lake. Surrounding this area are cultivated crops with cereals, such as *Triticum*
170 spp., as well as *Prunus dulcis* and *Olea europea*.

171 3 Material and methods

172 Two sediment cores, Padul-13-01 (37°00'40''N; 3°36'13''W) and Padul-15-05
173 (37°00'39.77''N; 3°36'14.06''W) with a length of 58.7 cm and 42.64 m, respectively, were
174 collected between 2013 and 2015 from the wetland (Fig. 1). The cores were taken using a
175 Rolatec RL-48-L drilling machine equipped with a hydraulic piston corer from the Scientific
176 Instrumentation Centre of the University of Granada (UGR). The sediment cores were
177 wrapped in film, put in core boxes, transported to UGR and stored in a dark cool room at 4°C.

178 3.1 Age-depth model (AMS radiocarbon dating)

179 The core chronology was constrained using fourteen AMS radiocarbon dates from plant
180 remains and organic bulk samples taken from the cores (Table 1). In addition, one sample
181 with gastropods was also submitted for AMS radiocarbon analysis, although it was rejected
182 due to important reservoir effect, that provided a very old date. Thirteen of these samples
183 came from Padul-15-05 with one from the nearby Padul-13-01 (Table 1). We were able to
184 use this date from Padul-13-01 core as there is a very significant correlation between the
185 upper part of Padul-15-05 and Padul-13-01 cores, shown by identical lithological and
186 geochemical changes (Supplementary information 1; Figure S1). The age model for the upper
187 ~3 m minus the upper 21 cm from the surface was built using the R-code package ‘Clam 2.2’

188 (Blaauw, 2010) employing the calibration curve IntCal 13 (Reimer et al., 2013), a 95 % of
189 confidence range, a smooth spline (type 4) with a 0.20 smoothing value and 1000 iterations
190 (Fig. 2). The chronology of the uppermost 21 cm of the record was built using a linear
191 interpolation between the last radiocarbon date and the top of the record (Present; 2015 CE).
192 Even though the length of the Padul-15-05 core is ~43 m, the studied interval in the work
193 presented here is the uppermost 115 cm of the record that are constrained by seven AMS
194 radiocarbon dates (Fig. 2).

195 3.2 Lithology, MS, XRF and TOC

196 Padul-15-05 core was split longitudinally and was described in the laboratory with respect to
197 lithology and color (Fig. 3). Magnetic susceptibility (MS) was measured with a Bartington
198 MS3 operating with a MS2E sensor. MS measurements (in SI units) were obtained directly
199 from the core surface every 0.5 cm (Fig. 3).

200
201 Elemental geochemical composition was measured in an X-Ray fluorescence (XRF)
202 Avaatech core scanner® at the University of Barcelona (Spain). A total of thirty-three
203 chemical elements were measured in the XRF core scanner at 10 mm of spatial resolution,
204 using 10 s count time, 10 kV X-ray voltage and a X-ray current of 650 μ A for lighter
205 elements and 35 s count time, 30 kV X-ray voltage, X-ray current of 1700 μ A for heavier
206 elements. Thirty-three chemical elements were measured but only the most representative
207 with a major number of counts were considered (Si, K, Ca, Ti, Fe, Zr, Br and Sr). Results for
208 each element are expressed as intensities in counts per second (cps) and normalized (norm.)
209 for the total sum in cps in every measure (Fig. 3).

210 Total organic carbon (TOC) was analyzed every 2 or 3 cm throughout the core. Samples were
211 previously decalcified with 1:1 HCl in order to eliminate the carbonate fraction. The
212 percentage of organic Carbon (OC %) was measured in an Elemental Analyzer Thermo
213 Scientific Flash 2000 model from the Scientific Instrumentation Centre of the UGR (Spain).
214 Percentage of TOC per gram of sediment was calculated from the percentage of organic
215 carbon (OC %) yielded by the elemental analyzer, and recalculated by the weight of the
216 sample prior to decalcification (Fig. 3).

217 3.3 Pollen and NPP

218 Samples for pollen analysis (1-3 cm³) were taken every 1 cm throughout the core, with a total
219 of 103 samples analyzes. Pollen extraction methods followed a modified Faegri and Iversen
220 (1989) methodology. Processing included the addition of *Lycopodium* spores for calculation
221 of pollen concentration. Sediment was treated with NaOH, HCl, HF and the residue was
222 sieved at 250 μ m previous to an acetolysis solution. Counting was performed using a
223 transmitted light microscope at 400 magnifications to an average pollen count of ca. 260
224 terrestrial pollen grains. Fossil pollen was identified using published keys (Beug, 2004) and
225 modern reference collections at University of Granada (Spain). Pollen counts were
226 transformed to pollen percentages based on the terrestrial pollen sum, excluding aquatics.
227 The palynological zonation was executed by cluster analysis using twelve primary pollen
228 taxa- *Olea*, *Pinus*, deciduous *Quercus*, evergreen *Quercus*, *Pistacia*, Ericaceae, *Artemisia*,
229 Asteroideae, Cichorioideae, Amaranthaceae and Poaceae (Grimm, 1987) (Fig. 4). Non-pollen
230 palynomorphs (NPP) include fungal and algal spores, and thecamoebians (testate amoebae).
231 The NPP percentages were calculated and represented with respect to the terrestrial pollen
232 sum (Fig. 4). Furthermore, some pollen taxa were grouped, according to present-day
233 ecological bases, into Mediterranean forest and xerophytes (Fig. 4). The Mediterranean forest

234 taxa is composed of *Quercus* total, *Olea*, *Phillyrea* and *Pistacia*. The xerophyte group
235 includes *Artemisia*, *Ephedra*, and *Amaranthaceae*.

236 **4 Results**

237 **4.1 Chronology and sedimentation rates**

238 The age-model of the upper 115 cm of Padul-15-05 core (Fig. 2) shows an average
239 sedimentation rate (SAR) of 0.058 cm/yr over last ~4700 cal yr BP, being the age constrained
240 by seven AMS ¹⁴C dates (Table 1). However, SARs of individual core segments vary from
241 0.01 to 0.16 cm/yr (Fig. 2), showing the lowest values between ~51 and 40 cm (from ~2600
242 to 1350 cal yr BP) and the highest values during the last ~20 cm (last century).

243 **4.2 Lithology, MS, XRF and TOC**

244 The stratigraphy of the upper ~115 cm of the Padul-15-05 sediment core was deduced
245 primarily by visual inspection. However, our visual inspections were support by comparison
246 with the element geochemical composition (XRF), the MS of the split cores, and TOC (Fig.
247 3) to determine shifts in sediment facies. The lithology for this sedimentary sequence consists
248 in clays with variable carbonates, siliciclastics and organic content (Fig. 3). We also used a
249 Linear r (Pearson) correlation to calculated relationship for the XRF data. The correlation for
250 the inorganic geochemical elements determined two different groups of elements that covary
251 (Table 2): Group 1) Si, K, Ti, Fe and Zr with a high positive correlation between them;
252 Group 2) Ca, Br and Sr have negative correlation with Group 1. Based on this, the sequence
253 is subdivided in two principal sedimentary units. The lower ~87 cm of the record is
254 designated to Unit 1, characterized principally by relatively low values of MS and higher
255 values of Ca. The upper ~28 cm of the sequence is designated to Unit 2, in which the
256 mineralogical composition is lower in Ca with higher values of MS in correlation with mostly
257 siliciclastics elements (Si, K, Ti, Fe and Zr).

258
259 Within these two units, four different facies can be identified by visual inspection and by the
260 elemental geochemical composition and TOC of the sediments. *Facies* 1 (115-110 cm depth,
261 ~4700 to 4650 cal yr BP; and 89-80 cm depth ~4300 to 4000 cal yr BP) are characterized by
262 dark brown organic clays that bear charophytes and macroscopic plant remains. They also
263 have depicted relative higher values of TOC values (Fig. 3). *Facies* 2 (110-89 cm depth
264 ~4650 to 4300 cal yr BP; and 80-42 cm depth, ~4000 to 1600 cal yr BP) is compose of brown
265 clays, with the occurrence of gastropods and charophytes. This facies is also characterized by
266 lower TOC values. *Facies* 3 (42-28 cm depth, ~1600 to 400 cal yr BP) is characterized by
267 grayish brown clays with the occurrence of gastropods, and lower values of TOC, and an
268 increasing trend in MS and in siliciclastic elements. *Facies* 4 (28-0 cm, ~400 cal yr BP to
269 Present) is made up of light grayish brown clays and features a strong increase in siliciclastic
270 linked to a strong increase in MS.

271 **4.3 Pollen and NPP**

272 Several terrestrial and aquatic pollen taxa were identified but only the most representative
273 taxa are here plotted in the summary pollen diagram (Fig. 4). Selected NPP percentages are
274 also displayed in Figure 4. Four pollen zones (PA) were visually identified with the help of a
275 cluster analysis using the program CONISS (Grimm, 1987). Pollen concentration was higher
276 during Unit 1 with a decreasing trend in the transition to Unit 2 and a later increase during the
277 pollen subzone PA-4b (Fig. 4). Pollen zones are described below:

278 **4.3.1 Zone PA-1 [~4720 to 3400 cal yr BP/ ~2800 to 1450 BCE (115-65 cm)]**

279 Zone 1 is characterized by the abundance of Mediterranean forest species reaching up to ca.
280 70 %. Another important taxon in this zone is *Pinus*, with average values around 18 %. Herbs
281 are largely represented by Poaceae, averaging around 10 %, and reaching up to ca. 25 %.
282 This pollen zone is subdivided into PA-1a, PA-1b and PA-1c (Fig. 4). The principal
283 characteristic that differentiating PA-1a from PA-1b (boundary at ~4650 cal yr BP/~2700
284 BCE) is the decrease in Poaceae, the increase in *Pinus*, and the appearance of cf. *Vitis*. The
285 subsequent decrease in Mediterranean forest pollen to average values around 40 %, the
286 increase in *Pinus* to average ~25 % and a progressive increase in Ericaceae to ~6 to 11 %,
287 distinguishes subzones PA-1b and PA-1c (boundary at ca. 3950 cal yr BP).

288 **4.3.2. Zone PA-2 [~3400 to 1550 cal yr BP/~1450 BCE to 400 CE (65-41 cm)]**

289 The main features of this zone are the increase in Ericaceae up to ~16 %, some herbs such as
290 Cichorioideae, became more abundant reaching average percentages of ~7 %. This pollen
291 zone can be subdivided in subzones PA-2a and PA-2b with a boundary at ~2850 cal yr BP
292 (~900 BCE). The principal characteristics that differentiate these subzones is marked by the
293 increasing trend in Ericaceae and deciduous *Quercus* reaching maximum values of ~30 %
294 and ~20 %, respectively. In addition, the increase in *Botryococcus*, which averages from ~4
295 to 9 %. Also notable is the expansion of *Mougeotia* and *Zygnema* types.

296 **4.3.3 Zone PA-3 [~1550 to 400 cal yr BP/~400 CE to 1550 CE (41-29 cm)]**

297 This zone is distinguished by the continuing decline of Mediterranean forest elements.
298 Cichorioideae reached average values of about 40 %, and is paralleled by the decrease in
299 Ericaceae. A decline in *Botryococcus* and other algal remains is also observed in this zone,
300 although there is an increase in total Thecamoebians from average of <1 % to 10 %. This
301 pollen zone is subdivided in subzones PA-3a and PA-3b at ~1000 cal yr BP (~950 CE). The
302 main features that differentiate these subzones are the increase in *Olea* from subzone PA-3a
303 to PA-3b from average values of ~1 to 5 %. The increasing trend in Poaceae is also a feature
304 in this subzone, as well as the slight increase in Asteroideae at the top. Significant changes
305 are documented in NPP percentages in this subzone with the increase of some fungal remain
306 such as *Tilletia* and *Glomus* type. Furthermore, a decrease in *Botryococcus* and the near
307 disappearance of other algal remains such as *Mougetia* occurred.

308 **4.3.4 Zone PA-4 [~last 400 cal yr BP/ ~ 1550 CE to Present (29-0 cm)]**

309 The main feature in this zone is the significant increase in *Pinus*, reaching maximum values
310 of ~32 %, an increase in Poaceae to ~40 %) and the decrease in Cichorioideae (~44 to 16 %).
311 Other important changes are the nearly total disappearance of some shrubs such as *Pistacia*
312 and a decreasing trend in Ericaceae, as well as a further decline in Mediterranean forest
313 pollen. An increase in wetland pollen taxa, mostly *Typha*, also occurred. A significant
314 increase in xerophytes, mostly Amaranthaceae to ~14 % is also observed in this period. Other
315 herbs such as *Plantago*, Polygonaceae and Convolvulaceae show moderate increases. PA-4 is
316 subdivided into subzones PA-4a and PA-4b (Fig. 4). The top of the record (PA-4b), which
317 corresponds with the last ~120 yr, is differentiated from subzone PA-4a (from ~400 – 120 cal
318 yr BP) by a decline in some herbs such as Cichorioideae. However, an increase in other herbs
319 such as Amaranthaceae and Poaceae occurred. The increase in *Plantago* is also significant
320 during this period. PA-4b also has a noteworthy increase in *Pinus* (from ~14 to 27 %) and a
321 slight increase in *Olea* and evergreen *Quercus* are also characteristic of this subzone. With

322 respect to NPPs, thecamoebians such as *Arcella* type and in the largely coprophilous
323 sordariaceous (Sordariales) spores also increase. This zone also documents the decrease in
324 fresh-water algal spores, in *Botryococcus* concomitant with *Mougeotia* and *Zygnema* type.

325 **4.4 Estimated lake level reconstruction**

326 Different local proxies from the Padul-15-05 record [Si, Ca, TOC, MS, hygrophytes
327 (Cyperaceae and *Typha*), Poaceae and algae (including *Botryococcus*, *Zygnema* types
328 and *Mougeotia*) groups] have been depicted in order to understand the relationship between
329 lithological, geochemical, and palynological variability and the water lake level oscillations.
330 Sediments with higher values of TOC (more algae and hygrophytes) and rich in Ca (related
331 with the occurrence of shells and charophytes remains) most likely characterized a shallow
332 water environment (Unit 1). The continuous decline in *Botryococcus*, the disappearance of
333 charophytes and the progressively increase in detritics (increase in MS and Si values) could
334 be associated with shallower and even ephemeral lake environment (transition from Unit 1 to
335 Unit 2; ~41 to 28 cm). The absence of aquatic remains, almost disappearance of
336 *Botryococcus* and decreasing Ca and a lower TOC and/or a higher input of clastic material
337 (higher MS and Si values) into the lake, could be related with lake level lowering, and even
338 emerged conditions (increase in Poaceae; Unit 2) (Fig. 5).

339 **4.5 Spectral analysis**

340 Spectral analysis was performed on selected pollen and NPP time series (Mediterranean
341 forest and *Botryococcus*), as well as TOC in order to identify millennial- and centennial-scale
342 periodicities. The mean sampling resolution for pollen and NPP is ~50 yr and for
343 geochemical data is ~80 yr. Statistically significant cycles, above the 90, 95 and 99 % of
344 confident levels, were found around 800, 680, 300, 240, 200, 170 (Fig. 7).

345 **5 Discussion**

346 Numerous proxies have been used in this study to interpret the paleoenvironmental and
347 hydrodynamic changes recorded in the Padul sedimentary record during the last 4700 cal yr
348 BP. Palynological analysis (pollen and NPP) is commonly used as a proxy for vegetation and
349 climate change, and lake level variations, as well as human impact and land uses (e.g. Faegri
350 and Iversen, 1990; van Geel et al., 1983). Disentangling natural vs. anthropogenic effects on
351 the environment in the last millennia is sometimes challenging but can be persuaded using a
352 multi-proxy approach (Roberts et al., 2011; Sadori et al., 2011). In this study, we used the
353 variations between Mediterranean forest taxa, xerophytes and algal communities for
354 paleoclimatic variability and the occurrence of nitrophilous and ruderal plant communities
355 and some NPPs for identifying human influence in the study area. Variations in arboreal
356 pollen (AP, including Mediterranean tree species) have previously been used in previous
357 Sierra Nevada records as a proxy for humidity changes (Jiménez-Moreno and Anderson,
358 2012; Ramos-Román et al., 2016). The increase or decrease in Mediterranean forest species
359 has been used as a proxy for climate change in other studies in the western Mediterranean
360 region, with greater forest development generally meaning higher humidity (Fletcher et al.,
361 2013; Fletcher and Sánchez-Goñi, 2008). On the other hand, increases in xerophyte pollen
362 taxa (i.e., *Artemisia*, *Ephedra*, Amaranthaceae) have been used as an indication of aridity in
363 this area (Anderson et al., 2011; Carrión et al., 2007).

364
365 The chlorophyceae alga *Botryococcus* sp. has been used as an indicator of freshwater
366 environments, in relatively productive fens, temporary pools, ponds or lakes (Guy-Ohlson,

367 1992). The high visual and statistical correlation between *Botryococcus* from Padul-15-05
368 and North Atlantic temperature estimations [Bond et al., 2001; $r = -0.63$; $p < 0.0001$; between
369 ca. 4700 to 1500 cal yr BP and $r = -0.48$; $p < 0.0001$ between 4700 and -65 cal yr BP (the
370 decreasing and very low *Botryococcus* occurrence in the last 1500 cal yr BP makes this
371 correlation moderate)] seems to show that in this case *Botryococcus* is driven by temperature
372 change and would reflect variations in lake productivity (increasing with warmer water
373 temperatures).

374

375 Human impact can be investigated using several palynomorphs. Nitrophilous and ruderal
376 pollen taxa, such as *Convolvulus*, *Plantago lanceolata* type, Urticaceae type and *Polygonum*
377 *avicularis* type, are often proxies for human impact (Riera et al., 2004), and abundant
378 Amaranthaceae has also been used as well (Sadori et al., 2003). Some species of
379 Cichorioideae have been described as nitrophilous taxa (Abel-Schaad and López-Sáez, 2013)
380 and as grazing indicators (Florenzano et al., 2015; Mercuri et al., 2006; Sadori et al., 2016).
381 At the same time, NPP taxa such as some coprophilous fungi, Sordariales and thecamoebians
382 are also used as indicators of anthropization and land use (Carrión et al., 2007; Ejarque et al.,
383 2015; van Geel et al., 1989; Riera et al., 2006). *Tilletia* a grass-parasitizing fungi has been
384 described as an indicator of grass cultivation in other Iberian records (Carrión et al., 2001a).
385 In this study we follow the example of others (van Geel et al., 1989; Morellón et al., 2016;
386 Sadori et al., 2016) who used the NPP soil mycorrhizal fungus *Glomus* sp. as a proxy for
387 erosive activity.

388

389 The palynological analysis, variations in the lithology, geochemistry and macrofossil remains
390 (gastropod shells and charophytes) from the Padul-15-05 core helped us reconstruct the
391 estimated lake level and the local environment changes in the Padul area and their
392 relationship with regional climate (Fig. 5). Several previous studies on Late Holocene lake
393 records from the Iberian Peninsula show that lithological changes can be used as a proxy for
394 lake level reconstruction (Martín-Puertas et al., 2011; Morellón et al., 2009; Riera et al.,
395 2004). For example, carbonate sediments formed by biogenic remains of gastropods and
396 charophytes are indicative of shallow lake waters (Riera et al., 2004). Furthermore, van Geel
397 et al. (1983), described occurrences of *Mougeotia* and *Zygnema* type (Zygnemataceae) as
398 typical of shallow water environments. The increase in organic matter accumulation deduced
399 by TOC (and Br) could be considered as characteristic of high productivity (Kalugin et al.,
400 2007) in these shallow water environments. On the other hand, increases in clastic input in
401 lake sediments have been interpreted as due to lowering of lake level and more influence of
402 terrestrial-fluvial deposition in a very shallow/ephemeral lake (Martín-Puertas et al., 2008).
403 Carrión (2002) related the increase in some fungal species and Asteraceae as indicators of
404 seasonal desiccation stages in lakes. Nevertheless, in natural environments with potential
405 interactions with human activities the increase in clastic deposition related with other
406 indications of soil erosion (e.g. *Glomus* sp.) may be assigned to intensification in land use
407 (Morellón et al., 2016; Sadori et al., 2016).

408 **5.1 Late Holocene aridification trend**

409 Our work confirms the progressive aridification trend that occurred during at least the last
410 ~4700 cal yr BP in the southern Iberian Peninsula, as shown here by the progressive decrease
411 in Mediterranean forest component and the increase in herbs (Figs. 4 and 6). Our lake level
412 interpretations agree with the pollen data, showing an overall decrease during the Late
413 Holocene, from a shallow water table containing relatively abundant organic matter (high
414 TOC, indicating higher productivity), gastropods and charophytes (high Ca values) to a low-

415 productive ephemeral/emerged environment (high clastic input and MS and decrease in Ca)
416 (Fig. 5). This natural progressive aridification confirmed by the decrease in Mediterranean
417 forest taxa and increase in siliciclastics pointing to a change towards ephemeral (even
418 emerged) environments became more prominent since about 1550 cal yr BP and then
419 enhanced again since ca. 400 cal yr BP to Present. A clear increase in human land use is also
420 observed during the last ca. 1550 cal yr BP (see below), including abundant *Glomus* from
421 erosion, which shows that humans were at least partially responsible for this sedimentary
422 change.

423 A suite of proxies previous studies supports our conclusions regarding the aridification trend
424 since the Middle Holocene (Carrión, 2002; Carrión et al., 2010; Fletcher et al., 2013; Fletcher
425 and Sánchez-Goñi, 2008; Jiménez-Espejo et al., 2014; Jiménez-Moreno et al., 2015). In the
426 western Mediterranean region the decline in forest development during the Middle and Late
427 Holocene is related with a decrease in summer insolation (Fletcher et al., 2013; Jiménez-
428 Moreno and Anderson, 2012), which may have decreased winter rainfall as a consequence of
429 a northward shift of the westerlies - a long-term enhanced positive NAO trend – which
430 induced drier conditions in this area since 6000 cal yr BP (Magny et al., 2012). Furthermore,
431 the decrease in summer insolation would produce a progressive cooling, with a reduction in
432 the length of the growing season as well as a decrease in the sea-surface temperature
433 (Marchal et al., 2002), generating a decrease in the land-sea contrast that would be reflected
434 in a reduction of the wind system and a reduced precipitation gradient from sea to shore
435 during the fall-winter season. The aridification trend can clearly be seen in the nearby alpine
436 records from the Sierra Nevada, where there was little influence by human activity (Anderson
437 et al., 2011; Jiménez-Moreno et al., 2013; Jiménez-Moreno and Anderson, 2012; Ramos-
438 Román et al., 2016).

439

440 **5.2 Millennial- and centennial-scale climate variability in the Padul area during the** 441 **Late Holocene**

442 The multi-proxy paleoclimate record from Padul-15-05 shows an overall aridification trend.
443 However, this trend seems to be modulated by millennial- and centennial-scale climatic
444 variability.

445 **5.2.1 Aridity pulses around 4200 (4500, 4300 and 4000 cal yr BP) and around 3000 cal** 446 **yr BP (3300 and 2800 cal yr BP)**

447 Marked aridity pulses are registered in the Padul-15-05 record around 4200 and 3000 cal yr
448 BP (Unit 1; PA-1 and PA-2a; Figs. 5 and 6). These arid pulses are mostly evidenced in this
449 record by declines in Mediterranean forest taxa, as well as lake level drops and/or cooling
450 evidenced by a decrease in organic component as TOC and the decrease in *Botryococcus*
451 algae. However, a discrepancy between the local and regional occurs between 3000-2800 cal
452 yr BP, with an increase in the estimated lake level and a decrease in the Mediterranean forest
453 during the late Bronze Age until the early Iron Age (Figs. 5 and 6). The disagreement could
454 be due to deforestation by humans during a very active period of mining in the area observed
455 as a peak in lead pollution in the alpine records from Sierra Nevada (García-Alix et al.,
456 2013). The aridity pulses agree regionally with recent studies carried out at higher in
457 elevation in the Sierra Nevada, a decrease in AP percentage in Borreguil de la Caldera record
458 around 4000-3500 cal yr BP (Ramos-Román et al., 2016), high percentage of non-arboreal
459 pollen around 3400 cal ka BP in Zoñar lake [Southern Córdoba Natural Reserve; (Martín-
460 Puertas et al., 2008)], and lake desiccation at ca. 4100 and 2900 cal yr BP in Lake Siles
461 (Carrión et al., 2007). Jalut et al. (2009) compared paleoclimatic records from different lakes

462 in the western Mediterranean region and also suggested a dry phase between 4300 to 3400 cal
463 yr BP, synchronous with this aridification phase. Furthermore, in the eastern Mediterranean
464 basin other pollen studies show a decrease in arboreal pollen concentration toward more open
465 landscapes around 4 cal ka BP (Magri, 1999).

466
467 Significant climatic changes also occurred in the Northern Hemisphere at those times and
468 polar cooling and tropical aridity are observed at ca. 4200-3800 and 3500-2500 cal yr BP;
469 (Mayewski et al., 2004), cold events in the North Atlantic [cold event 3 and 2; (Bond et al.,
470 2001)], decrease in solar irradiance (Steinhilber et al., 2009) and humidity decreases in the
471 eastern Mediterranean area at 4200 cal yr BP (Bar-Matthews et al., 2003) that could be
472 related with global scale climate variability (Fig. 6). These generally dry phases between 4.5
473 and 2.8 in Padul-15-05 are generally in agreement with persistent positive NAO conditions
474 during this time (Olsen et al., 2012).

475 The high-resolution Padul-15-05 record shows that climatic crises such as the essentially
476 global event at ~4200 cal yr BP (Booth et al., 2005), are actually multiple events in climate
477 variability at centennial-scales (i.e., ca. 4500, 4300, 4000 cal yr BP).

478 **5.2.2 Iberian-Roman Humid Period (~2600 to 1600 cal yr BP)**

479 High relative humidity is recorded in the Padul-15-05 record between ca. 2600 and 1600 cal
480 yr BP, synchronous with the well-known Iberian-Roman Humid Period (IRHP; between 2600
481 and 1600 cal yr BP; (Martín-Puertas et al., 2009). This is interpreted in our record due to an
482 increase in the Mediterranean forest species at that time (Unit 1; PA-2b; Figs. 6). In addition,
483 there is a simultaneous increase in *Botryococcus* algae, which is probably related to higher
484 productivity during warmer conditions and relatively higher water level. A minimum in
485 sedimentary rates at this time is also recorded, probably related with lower detritic input
486 caused by less erosion due to afforestation and probably also related to the decrease in TOC
487 due to less organic accumulation in the sediment. Evidence of a wetter climate around this
488 period has also been shown in several alpine records from Sierra Nevada. For example, in the
489 Laguna de la Mula core (Jiménez-Moreno et al. 2013) an increase in deciduous *Quercus* is
490 correlated with the maximum in algae between 2500 to 1850 cal yr BP, also evidencing the
491 most humid period of the Late Holocene. A geochemical study from the Laguna de Río Seco
492 (also in Sierra Nevada) also evidenced humid conditions around 2200 cal yr BP by the
493 decrease in Saharan dust input and the increase in detritic sedimentation into the lake
494 suggesting higher rainfall (Jiménez-Espejo et al., 2014). In addition, Ramos-Román et al.
495 (2016) showed an increase in AP in the Borreguil de la Caldera record around 2200 cal yr
496 BP, suggesting an increase in humidity at that time.

497
498 Other records from the Iberian Peninsula also show this pattern to wetter conditions during
499 the IRHP. For example, high lake levels are recorded in Zoñar Lake in southern Spain
500 between 2460 to 1600 cal yr BP, only interrupted by a relatively arid pulse between 2140 and
501 1800 cal yr BP (Martín-Puertas et al., 2009). An increase in rainfall is described in the central
502 region of the Iberian Peninsula in a study from the Tablas de Daimiel National Park between
503 2100 and 1680 cal yr BP (Gil García et al., 2007). Deeper lake levels at around 2650 to 1580
504 cal yr BP, also interrupted by an short arid event at ca. 2125-1790 cal yr BP, were observed
505 to the north, in the Iberian Range (Currás et al., 2012). The fact that the Padul-15-05 record
506 also shows a relatively arid-cold event between 2150-2050 cal yr BP, just in the middle of
507 this relative humid-warm period, seems to point to a common feature of centennial-scale
508 climatic variability in many western Mediterranean and North Atlantic records (Fig. 6).
509 Humid climate conditions at around 2500 cal yr BP are also interpreted in previous studies

510 from lake level reconstructions from Central Europe (Magny, 2004). Increases in temperate
511 deciduous forest are also observed in marine records from the Alboran Sea around 2600 to
512 2300 cal yr BP, also pointing to high relative humidity (Combourieu-Nebout et al., 2009).
513 Overall humid conditions between 2600 and 1600 cal yr BP seem to agree with predominant
514 negative NAO reconstructions at that time, which would translate into greater winter (and
515 thus more effective) precipitation in the area triggering greater development of forest species
516 in the area.

517

518 Generally warm conditions are interpreted between 1900 and 1700 cal yr BP in the
519 Mediterranean Sea, with high sea surface temperatures (SSTs), and in the North Atlantic
520 area, with the decrease in Drift Ice Index. In addition, persistent positive solar irradiance
521 occurred at that time. The increase in *Botryococcus* algae reaching maxima during the IRHP
522 also seems to point to very productive and perhaps warmer conditions in the Padul area (Fig.
523 6). There seems to be a short lag of about 200 years between maximum in *Botryococcus* and
524 maximum in Mediterranean forest. This could be due to different speed of reaction to climate
525 change, with algae (short life cycle, blooming if conditions are favorable) responding faster
526 than forest (tree development takes decades). An alternative explanation could be that they
527 might be responding to different forcings, with regional signal (forest) mostly conditioned by
528 precipitation and local (algae) also conditioned by temperature (productivity).

529 **5.2.3 DA and MCA (~1550 cal yr BP to 600 cal yr BP)**

530 Enhanced aridity occurred right after the IRHP in the Padul area. This is deduced in the
531 Padul-15-05 record by a significant forest decline, with a prominent decrease in
532 Mediterranean forest elements, an increase in herbs (Unit 1; PA-3; Figs. 4 and 6). In addition,
533 our evidence suggests a transition from a shallow lake to a more ephemeral wetland. This is
534 suggested by the disappearance of charophytes, a significant decrease in algae component
535 and higher Si and MS and lower TOC values (Unit 1; Figs. 5). Humans probably also
536 contributed to enhancing erosion in the area during this last ~1550 cal yr BP. The significant
537 change during the transition from Unit 1 to Unit 2 with a decrease in the pollen concentration
538 and the increase in Cichoroideae could be due to enhanced pollen degradation as
539 Cichoroideae have been found to be very resistant to pollen deterioration (Bottema, 1975).
540 However, the occurrence of other pollen taxa (e.g. *Quercus*, Ericaceae, *Pinus*, Poaceae, *Olea*)
541 showing climatic trends and increasing between ca. 1500-400 cal yr BP and a decrease in
542 Cichoroideae in the last ~400 cal yr BP, when an increase in clastic material occurred, do not
543 entirely support a preservation issue (see section of Human activity; 5.4).

544

545 This phase could be separated into two different periods. The first period occurred between
546 ~1550 cal yr BP and 1100 cal yr BP (~400 to 900 CE) and is characterized by a decreasing
547 trend in Mediterranean forest and *Botryococcus* taxa. This period corresponds with the Dark
548 Ages [from ca. 500 to 900 CE; (Moreno et al., 2012)]. Correlation between the decline in
549 Mediterranean forest, the increase in the Drift Ice Index in the North Atlantic record (cold
550 event 1; Bond et al., 2001), the decline in SSTs in the Mediterranean Sea and maxima in
551 positive NAO reconstructions suggests drier and colder conditions during this time (Fig. 6).
552 Other Mediterranean and central-European records agree with our climate interpretations, for
553 example, a decrease in forest pollen types is shown in a marine record from the Alboran Sea
554 (Fletcher et al., 2013) and a decrease in lake levels is also observed in Central Europe
555 (Magny et al., 2004) pointing to aridity during the DA. Evidences of aridity during the DA
556 have been shown too in the Mediterranean part of the Iberian Peninsula, for instance, cold
557 and arid conditions were suggested in the northern Betic Range by the increase in xerophytic

558 herbs around 1450 and 750 cal yr BP (Carrión et al., 2001b) and in southeastern Spain by a
559 forest decline in lacustrine deposits around 1620 and 1160 cal yr BP (Carrión et al., 2003).
560 Arid and colder conditions during the Dark Ages (around 1680 to 1000 cal yr BP) are also
561 suggested for the central part of the Iberian Peninsula using a multiproxy study of a sediment
562 record from the Tablas de Daimiel Lake (Gil García et al., 2007).

563

564 A second period that we could differentiate occurred around 1100 to 600 cal yr BP/900 to
565 1350 CE, during the well-known MCA (900 to 1300 CE after Moreno et al., 2012). During
566 this period the Padul-15-05 record shows a slight increasing trend in the Mediterranean forest
567 taxa with respect to the DA, but the decrease in *Botryococcus* and the increase in herbs still
568 point to overall arid conditions. This change could be related to an increase in temperature,
569 favoring the development of temperate forest species, and would agree with inferred
570 increasing temperatures in the North Atlantic areas, as well as the increase in solar irradiance
571 and the increase in SSTs in the Mediterranean Sea (Fig. 6). This hypothesis would agree with
572 the reconstruction of persistent positive NAO and overall warm conditions during the MCA
573 in the western Mediterranean (see synthesis in Moreno et al., 2012). A similar pattern of
574 increasing xerophytic vegetation during the MCA is observed in alpine peat bogs and lakes in
575 the Sierra Nevada (Anderson et al., 2011; Jiménez-Moreno et al., 2013; Ramos-Román et al.,
576 2016) and arid conditions are shown to occur during the MCA in southern and eastern Iberian
577 Peninsula deduced by increases in salinity and lower lake levels (Corella et al., 2013; Martín-
578 Puertas et al., 2011). However, humid conditions have been reconstructed for the
579 northwestern of the Iberian Peninsula at this time (Lebreiro et al., 2006; Moreno et al., 2012),
580 as well as northern Europe (Martín-Puertas et al., 2008). The different pattern of precipitation
581 between northwestern Iberia / northern Europe and the Mediterranean area is undoubtedly a
582 function of the NAO precipitation dipole (Trouet et al., 2009).

583 **5.2.4 The last ~600 cal yr BP: LIA (~600 to 100 cal yr BP/~1350 to 1850 CE) and IE** 584 **(~100 cal yr BP to Present/~1850 CE-Present)**

585 Two climatically distinct periods can be distinguished during the last ca. 600 years (end of
586 PA-3b to PA-4; Fig. 4) in the area. However, the climatic signal is more difficult to interpret
587 due to a higher human impact at that time. The first phase around 600-500 cal yr BP was
588 characterized as increasing relative humidity by the decrease in xerophytes and the increase
589 in Mediterranean forest taxa and *Botryococcus* after a period of decrease during the DA and
590 MCA, corresponding to the LIA. The second phase is characterized here by the decrease in
591 the Mediterranean forest around 300-100 cal yr BP, pointing to a return to more arid
592 conditions during the last part of the LIA (Figs. 5 and 6). This climatic pattern agrees with an
593 increase in precipitation by the transition from positive to negative NAO mode and from
594 warmer to cooler conditions in the North Atlantic area during the first phase of the LIA and a
595 second phase characterized by cooler (cold event 0; Bond et al., 2001) and drier conditions
596 (Fig. 6). A stronger variability in the SSTs is described in the Mediterranean Sea during the
597 LIA (Fig. 6). Mayewski et al. (2004) described a period of climate variability during the
598 Holocene at this time (600 to 150 cal yr BP) suggesting a polar cooling but more humid in
599 some parts of the tropics. Regionally, (Morellón et al., 2011) also described a phase of more
600 humid conditions between 1530 to 1750 CE (420 to 200 cal yr BP) in a lake sediment record
601 from NE Spain. An alternation between wetter to drier periods during the LIA are also shown
602 in the nearby alpine record from Borreguil de la Caldera in the Sierra Nevada mountain range
603 (Ramos-Román et al., 2016).

604 The environmental transition from ephemeral, observed in the last ca. 1550 cal yr BP (Unit 1;
605 Fig. 5), to emerged conditions occur in the last ca. 400 cal yr BP. This is shown by the

606 highest MS and Si values, enhance sedimentation rates and the increase in wetland plants and
607 the stronger decrease in Ca and organic components (TOC) in the sediments in the uppermost
608 part of the Padul-15-05 record (Unit 2; Figs. 3 and 5).

609 **5.3 Centennial-scale variability**

610 Time series analysis has become important in determining the recurrent periodicity of
611 cyclical oscillations in paleoenvironmental sequences (e.g. Jiménez-Espejo et al., 2014;
612 Ramos-Román et al., 2016; Rodrigo-Gámiz et al., 2014; Fletcher et al., 2013). This analysis
613 also assists in understanding possible relationships between the paleoenvironmental proxy
614 data and the potential triggers of the observed cyclical changes: i.e., solar activity,
615 atmospheric, oceanic dynamics and climate evolution during the Holocene. The
616 cyclostratigraphic analysis on the pollen (Mediterranean forest; regional signal), algae
617 (*Botryococcus*; local signal) and TOC (local signal) times series from the Padul-15-05 record
618 evidence centennial-scale cyclical patterns with periodicities around ~800, 680, 300, 240, 200
619 and 170 years above the 90 % confidence levels (Fig. 7).

620
621 Previous cyclostratigraphic analysis in Holocene western Mediterranean records suggest
622 cyclical climatic oscillations with periodicities around 1500 and 1750 yr (Fletcher et al.,
623 2013; Jiménez-Espejo et al., 2014; Rodrigo-Gámiz et al., 2014). Other North Atlantic and
624 Mediterranean records also present cyclicities in their paleoclimatic proxies of ca. 1600 yr
625 (Bond et al., 2001; Debret et al., 2007; Rodrigo-Gámiz et al., 2014). However, this cycle is
626 absent from the cyclostratigraphic analysis in the Padul-15-05 record (Fig. 7). In contrast, the
627 spectral analysis performed in the Mediterranean forest time series from Padul record,
628 pointing to cyclical hydrological changes, shows a significant ~800 yr cycle that could be
629 related to solar variability (Damon and Sonett, 1991) or could be the second harmonic of the
630 ca. ~1600 yr oceanic-related cycle (Debret et al., 2009). A very similar periodicity of ca. 760
631 yr is detected in the *Pinus* forest taxa, also pointing to humidity variability, from the alpine
632 Sierra Nevada site of Borreguil de la Caldera and seems to show that this is a common
633 feature of cyclical paleoclimatic oscillation in the area.

634
635 A significant ~680 cycle is shown in the *Botryococcus* time series most likely suggesting
636 recurrent centennial-scale changes in temperature (productivity) and water availability. A
637 similar cycle is shown in the *Artemisia* signal in an alpine record from Sierra Nevada
638 (Ramos-Román et al., 2016). This cycle around ~650 yr is also observed in a marine record
639 from the Alboran Sea, and was interpreted as the secondary harmonic of the 1300 yr cycle
640 that those authors related with cyclic thermohaline circulation and sea surface temperature
641 changes (Rodrigo-Gámiz et al., 2014).

642
643 A statistically significant ~300 yr cycle is shown in the Mediterranean forest taxa and TOC
644 from the Padul-15-05 record suggesting shorter-scale variability in water availability. This
645 cycle is also observed in the cyclical *Pinus* pollen data from Borreguil de la Caldera at higher
646 elevations in the Sierra Nevada (Ramos-Román et al., 2016). This cycle could be principally
647 related to NAO variability as observed by Olsen et al. (2012), which follows variations in
648 humidity observed in the Padul-15-05 record. NAO variability also regulates modern
649 precipitation in the area.

650
651 The *Botryococcus* and TOC time series shows variability with a periodicity around ~240, 200
652 and 164 yrs. Sonett and Suess, (1984) described a significant cycle in solar activity around
653 ~208 yr (Suess solar cycle), which could have triggered our ~200 cyclicity. The observed

654 ~240 yr periodicity in the Padul-15-05 record could be either related to variations in solar
655 activity or due to the mixed effect of the solar together with the ~300 yr NAO-interpreted
656 cycle and could point to a solar origin of the centennial-scale NAO variations as suggested by
657 previously published research (Lukianova and Alekseev, 2004; Zanchettin et al., 2008).
658 Finally, a significant ~170 yr cycle has been observed in both the Mediterranean forest taxa
659 and *Botryococcus* times series from the Padul-15-05 record. A similar cycle (between 168-
660 174 yr) was also described in the alpine pollen record from Borreguil de la Caldera in Sierra
661 Nevada (Ramos-Román et al., 2016), which shows that it is a significant cyclical pattern in
662 climate, probably precipitation, in the area. This cycle could be related to the previously
663 described ~170 yr cycle in the NAO index (Olsen et al., 2012), which would agree with the
664 hypothesis of the NAO controlling millennial- and centennial-scale environmental variability
665 during the Late Holocene in the area (García-Alix et al., 2017; Ramos-Román et al., 2016).

666 **5.4 Human activity**

667 Humans probably had an impact in the area since Prehistoric times, however, the Padul-15-05
668 multiproxy record shows a more significant human impact during the last ca. 1550 cal yr BP,
669 which intensified in the last ~500 years (since 1450 CE to Present). This is deduced by, a
670 significant increase in nitrophilous plant taxa such as Cichorioideae, Convolvulaceae,
671 Polygonaceae and *Plantago* and the increase in some NPP such as *Tilletia*, coprophilous
672 fungi and thecamoebians (Unit 2; PA-4; Fig. 4). Most of these pollen taxa and NPPs are
673 described in other southern Iberian paleoenvironmental records as indicators of land uses, for
674 instance, *Tilletia* and covarying nitrophilous plants have been described as indicators of
675 farming (e.g. Carrión et al., 2001a). Thecamoebians also show a similar trend and have also
676 been detected in other areas being related to nutrient enrichment as consequences of livestock
677 (Fig. 8). The stronger increase in Cichorioideae have also been described as indicators of
678 animal grazing in areas subjected to intense use of the territory (Mercuri et al., 2006).
679 Interestingly, these taxa began to decline around ca. 400 cal yr BP (~1550 CE), coinciding
680 with the higher increase in detritic material into the basin. We could then interpreted this
681 increase in Cichorioideae as greater in livestock activity in the surroundings of the lake
682 during this period, which is supported by the increase in these other proxies related with
683 animal husbandry.

684
685 Climatically, this event coincides with the start of persistent negative NAO conditions in the
686 area (Trouet et al., 2009), which could have further triggered more rainfall and more detritic
687 input into the basin. (Bellin et al., 2011) in a study from the Betic Cordillera (southern Iberian
688 Peninsula) demonstrate that soil erosion increase in years with higher rainfall and this could
689 be intensified by human impact. Nevertheless, in a study in the southeastern part of the
690 Iberian Peninsula (Bellin et al., 2013) suggested that major soil erosion could have occurred
691 by the abandonment of agricultural activities in the mountain areas as well as the
692 abandonment of irrigated terrace systems during the Christian Reconquest. Enhanced soil
693 erosion at this time is also supported by the increase in *Glomus* type (Figs. 4 and 8).

694
695 An important change in the sedimentation in the environment is observed during the last ca.
696 400 cal yr BP marked by the stronger increase in MS and Si values. This higher increase in
697 detritics occurred during an increase in other plants related with human and land uses such as
698 Polygonaceae, Amaranthaceae, Convolvulaceae, *Plantago*, Apiaceae and Cannabaceae-
699 Urticaceae type (Land Use Plants; Fig. 8). This was probably related to drainage canals in the
700 Padul wetland in the late XVIII century for cultivation purposes (Villegas Molina, 1967). The
701 increase in wetland vegetation and higher values of Poaceae could be due to cultivation of

702 cereals or by an increase in the population of *Phragmites australis* (also a Poaceae), very
703 abundant in the Padul lake margins at present due to the increase in drained land surface.
704 The uppermost part (last ca. 100 cal yr BP) of the pollen record from Padul-15-05 shows an
705 increasing trend in some arboreal taxa at that time, including Mediterranean forest, *Olea* and
706 *Pinus* (Fig. 4). This change is most likely of human origin and generated by the increase in
707 *Olea* cultivation in the last two centuries, also observed in many records from higher
708 elevation sites from Sierra Nevada, and *Pinus* and other Mediterranean species reforestation
709 in the 20th century (Anderson et al., 2011; Jiménez-Moreno and Anderson, 2012; Jiménez-
710 Moreno et al., 2013; Ramos-Román et al., 2016).

711 **6 Conclusions**

712 Our multiproxy analysis from the Padul-15-05 sequence has provided a detailed climate
713 reconstruction for the last 4700 ca yr BP for the Padul area and the western Mediterranean.
714 This study, supported by the comparison with other Mediterranean and North Atlantic
715 records suggests a link between vegetation, atmospheric dynamics and insolation and solar
716 activity during the Late Holocene. A climatic aridification trend occurred during the Late
717 Holocene in the Sierra Nevada and the western Mediterranean, probably linked with an
718 orbital-scale declining trend in summer insolation. This long-term trend is modulated by
719 centennial-scale climate variability as shown by the pollen (Mediterranean forest taxa), algae
720 (*Botryococcus*) and sedimentary and geochemical data in the Padul record. These events can
721 be correlated with regional and global scale climate variability. Cold and arid pulses
722 identified in this study around the 4200 and 3000 cal yr BP are synchronous with cold events
723 recorded in the North Atlantic and decreases in precipitation in the Mediterranean area,
724 probably linked to persistent positive NAO mode. Moreover, one of the most important
725 humid and warmer periods during the Late Holocene in the Padul area coincides in time with
726 the well-known IRHP, characterized by warm and humid conditions in the Mediterranean and
727 North Atlantic regions and overall negative NAO conditions. A drastic decline in
728 Mediterranean forest taxa, trending towards an open landscape and pointing to colder
729 conditions with enhanced aridity, occurred in two steps (DA and end of the LIA) during the
730 last ~1550 cal yr BP. However, this trend was slightly superimposed by a more arid but
731 warmer event coinciding with the MCA and a cold but wetter event during the first part of the
732 LIA. Besides natural climatic and environmental variability, strong evidences exists for
733 intense human activities in the area during the last ~1550 years. This suggests that the natural
734 aridification trend during the Late Holocene, which produced a progressive decrease in the
735 Mediterranean forest taxa in the Padul area, could have been intensified by human activities,
736 notably in the last centuries.
737 Furthermore, time series analyses done in the Padul-15-05 record show centennial-scale
738 changes in the environment and climate that are coincident with the periodicities observed in
739 solar, oceanic and NAO reconstructions and could show a close cause-and-effect linkage
740 between them.

741 **Acknowledgements**

742 This work was supported by the project P11-RNM-7332 funded by Consejería de Economía,
743 Innovación, Ciencia y Empleo de la Junta de Andalucía, the project CGL2013-47038-R
744 funded by Ministerio de Economía y Competitividad of Spain and fondo Europeo de
745 desarrollo regional FEDER and the research group RNM0190 (Junta de Andalucía). M. J. R.-
746 R. acknowledges the PhD funding provided by Consejería de Economía, Innovación, Ciencia
747 y Empleo de la Junta de Andalucía (P11-RNM-7332). J.C. acknowledges the PhD funding
748 provided by Ministerio de Economía y Competitividad (CGL2013-47038-R). A.G.-A. was

749 also supported by a Ramón y Cajal Fellowship RYC-2015-18966 of the Spanish Government
750 (Ministerio de Economía y Competividad). Javier Jaimez (CIC-UGR) is thanked for
751 graciously helping with the coring, the drilling equipment and logistics. We also would like
752 to thanks to the editor (Nathalie Combourieu-Nebout) and Graciela Gil-Romera, Laura
753 Sadori and an anonymous reviewer for their comments and suggestions which improved the
754 manuscript.

755 **References**

- 756 Abel-Schaad, D. and López-Sáez, J. A.: Vegetation changes in relation to fire history and
757 human activities at the Peña Negra mire (Bejar Range, Iberian Central Mountain System,
758 Spain) during the past 4,000 years, *Veg. Hist. Archaeobotany*, 22(3), 199–214,
759 doi:10.1007/s00334-012-0368-9, 2013.
- 760 Alfaro, P., Galinod-Zaldievar, J., Jabaloy, A., López-Garrido, A. C. and Sanz de Galdeano,
761 C.: Evidence for the activity and paleoseismicity of the Padul fault (Betic Cordillera,
762 Southern Spain) [Evidencias de actividad y paleosismicidad de la falla de Padul (Cordillera
763 Bética, sur de España)], *Acta Geol. Hisp.*, 36(3–4), 283–297, 2001.
- 764 Alpert, P., Baldi, M., Ilani, R., Krichak, S., Price, C., Rodó, X., Saaroni, H., Ziv, B., Kishcha,
765 P., Barkan, J., Mariotti, A. and Xoplaki, E.: Chapter 2 Relations between climate variability
766 in the Mediterranean region and the tropics: ENSO, South Asian and African monsoons,
767 hurricanes and Saharan dust, *Dev. Earth Environ. Sci.*, 4(C), 149–177, doi:10.1016/S1571-
768 9197(06)80005-4, 2006.
- 769 Anderson, R. S., Jiménez-Moreno, G., Carrión, J. S. and Pérez-Martínez, C.: Postglacial
770 history of alpine vegetation, fire, and climate from Laguna de Río Seco, Sierra Nevada,
771 southern Spain, *Quat. Sci. Rev.*, 30(13–14), 1615–1629,
772 doi:https://doi.org/10.1016/j.quascirev.2011.03.005, 2011.
- 773 Bar-Matthews, M., Ayalon, A., Gilmour, M., Matthews, A. and Hawkesworth, C. J.: Sea-
774 land oxygen isotopic relationships from planktonic foraminifera and speleothems in the
775 Eastern Mediterranean region and their implication for paleorainfall during interglacial
776 intervals, *Geochim. Cosmochim. Acta*, 67(17), 3181–3199,
777 doi:https://doi.org/10.1016/S0016-7037(02)01031-1, 2003.
- 778 Bellin, N., Vanacker, V., van Wesemael, B., Solé-Benet, A. and Bakker, M. M.: Natural and
779 anthropogenic controls on soil erosion in the internal betic Cordillera (southeast Spain),
780 *Catena*, 87(2), 190–200, doi:10.1016/j.catena.2011.05.022, 2011.
- 781 Bellin, N., Vanacker, V. and De Baets, S.: Anthropogenic and climatic impact on Holocene
782 sediment dynamics in SE Spain: A review, *Quat. Int.*, 308–309, 112–129,
783 doi:10.1016/j.quaint.2013.03.015, 2013.
- 784 Beug, H.-J.: Leitfaden der Pollenbestimmung für Mitteleuropa und angrenzende Gebiete,
785 *Fisch. Stuttg.*, 61, 2004.
- 786 Blaauw, M.: Methods and code for ‘classical’ age-modelling of radiocarbon sequences, *Quat.*
787 *Geochronol.*, 5(5), 512–518, doi:https://doi.org/10.1016/j.quageo.2010.01.002, 2010.
- 788 Bond, G., Kromer, B., Beer, J., Muscheler, R., Evans, M. N., Showers, W., Hoffmann, S.,
789 Lotti-Bond, R., Hajdas, I. and Bonani, G.: Persistent Solar Influence on North Atlantic
790 Climate During the Holocene, *Science*, 294(5549), 2130, doi:10.1126/science.1065680,
791 2001.
- 792 Booth, R. K., Jackson, S. T., Forman, S. L., Kutzbach, J. E., E. A. Bettis, I., Kreigs, J. and
793 Wright, D. K.: A severe centennial-scale drought in midcontinental North America 4200
794 years ago and apparent global linkages, *The Holocene*, 15(3), 321–328,
795 doi:10.1191/0959683605hl825ft, 2005.

- 796 Bottema, S.: The interpretation of pollen spectra from prehistoric settlements (with special
797 attention of Liguliflorae), *Palaeohistoria*, 17, 17–35, 1975.
- 798 Carrión, J. S.: Patterns and processes of Late Quaternary environmental change in a montane
799 region of southwestern Europe, *Quat. Sci. Rev.*, 21(18–19), 2047–2066,
800 doi:[https://doi.org/10.1016/S0277-3791\(02\)00010-0](https://doi.org/10.1016/S0277-3791(02)00010-0), 2002.
- 801 Carrión, J. S., Munuera, M., Dupré, M. and Andrade, A.: Abrupt vegetation changes in the
802 Segura Mountains of southern Spain throughout the Holocene, *J. Ecol.*, 89(5), 783–797,
803 doi:10.1046/j.0022-0477.2001.00601.x, 2001b.
- 804 Carrión, J. S., Andrade, A., Bennett, K. D., Navarro, C. and Munuera, M.: Crossing forest
805 thresholds: inertia and collapse in a Holocene sequence from south-central Spain, *The*
806 *Holocene*, 11(6), 635–653, doi:10.1191/09596830195672, 2001a.
- 807 Carrión, J. S., Fernández, S., Jiménez-Moreno, G., Fauquette, S., Gil-Romera, G., González-
808 Sampériz, P. and Finlayson, C.: The historical origins of aridity and vegetation degradation in
809 southeastern Spain, *J. Arid Environ.*, 74(7), 731–736,
810 doi:<https://doi.org/10.1016/j.jaridenv.2008.11.014>, 2010a.
- 811 Carrión, J. S., Sánchez-Gómez, P., Mota, J. F., Yll, R. and Chaín, C.: Holocene vegetation
812 dynamics, fire and grazing in the Sierra de Gádor, southern Spain, *Holocene*, 13(6), 839–849,
813 doi:10.1191/0959683603hl662rp, 2003.
- 814 Carrión, J. S., Fuentes, N., González-Sampériz, P., Quirante, L. S., Finlayson, J. C.,
815 Fernández, S. and Andrade, A.: Holocene environmental change in a montane region of
816 southern Europe with a long history of human settlement, *Quat. Sci. Rev.*, 26(11–12), 1455–
817 1475, doi:<https://doi.org/10.1016/j.quascirev.2007.03.013>, 2007.
- 818 Castillo Martín, A., Benavente Herrera, J., Fernández Rubio, R. and Pulido Bosch, A.:
819 Evolución y ámbito hidrogeológico de la laguna de Padul (Granada), *Las Zonas Húmedas En*
820 *Andal. Monogr. DGMA-MOPU*, 1984.
- 821 Combourieu-Nebout, N., Peyron, O., Dormoy, I., Desprat, S., Beaudouin, C., Kotthoff, U.
822 and Marret, F.: Rapid climatic variability in the west Mediterranean during the last 25 000
823 years from high resolution pollen data, *Clim Past*, 5(3), 503–521, doi:10.5194/cp-5-503-
824 2009, 2009.
- 825 Corella, J. P., Stefanova, V., El Anjoumi, A., Rico, E., Giralt, S., Moreno, A., Plata-Montero,
826 A. and Valero-Garcés, B. L.: A 2500-year multi-proxy reconstruction of climate change and
827 human activities in northern Spain: The Lake Arreo record, *Palaeogeogr. Palaeoclimatol.*
828 *Palaeoecol.*, 386, 555–568, doi:10.1016/j.palaeo.2013.06.022, 2013.
- 829 Currás, A., Zamora, L., Reed, J. M., García-Soto, E., Ferrero, S., Armengol, X., Mezquita-
830 Joanes, F., Marqués, M. A., Riera, S. and Julià, R.: Climate change and human impact in
831 central Spain during Roman times: High-resolution multi-proxy analysis of a tufa lake record
832 (Somolinos, 1280m asl), *Catena*, 89(1), 31–53, doi:10.1016/j.catena.2011.09.009, 2012.
- 833 Damon, P. E. and Sonett, C. P.: Solar and terrestrial components of the atmospheric C-14
834 variation spectrum. In: Sonett, C.P., Giampapa, M.S., Matthews, M.S. (Eds.), *The Sun in*
835 *Time*. University of Arizona Press, Tucson, AZ, USA., 1991.

- 836 Debret, M., Bout-Roumazeilles, V., Grousset, F., Desmet, M., McManus, J. F., Massei, N.,
837 Sebag, D., Petit, J.-R., Copard, Y. and Trentesaux, A.: The origin of the 1500-year climate
838 cycles in holocene north-atlantic records, *Clim. Past*, 3(4), 569–575, 2007.
- 839 Debret, M., Sebag, D., Crosta, X., Massei, N., Petit, J.-R., Chapron, E. and Bout-
840 Roumazeilles, V.: Evidence from wavelet analysis for a mid-Holocene transition in global
841 climate forcing, *Quat. Sci. Rev.*, 28(25–26), 2675–2688,
842 doi:<https://doi.org/10.1016/j.quascirev.2009.06.005>, 2009.
- 843 Delgado, J., Alfaro, P., Galindo-Zaldivar, J., Jabaloy, A., Lopez Garrido, A. and Sanz de
844 Galdeano, C.: Structure of the Padul-Nigüelas basin (S Spain) from H/V ratios of ambient
845 noise: application of the method to study peat and coarse sediments, *Pure Appl. Geophys.*,
846 159(11), 2733–2749, 2002.
- 847 Domingo-García, M., Fernández-Rubio, R., Lopez, J. and González, C.: Aportación al
848 conocimiento de la Neotectónica de la Depresión del Padul (Granada), *Tecniterrae*, 53, 6–16,
849 1983.
- 850 Ejarque, A., Anderson, R. S., Simms, A. R. and Gentry, B. J.: Prehistoric fires and the
851 shaping of colonial transported landscapes in southern California: A paleoenvironmental
852 study at Dune Pond, Santa Barbara County, *Quat. Sci. Rev.*, 112, 181–196,
853 doi:<https://doi.org/10.1016/j.quascirev.2015.01.017>, 2015.
- 854 El Aallali, A., Nieto, J. M. L., Raya, F. A. P. and Mesa, J. M.: Estudio de la vegetación
855 forestal en la vertiente sur de Sierra Nevada (Alpujarra Alta granadina), *Itinera Geobot.*, (11),
856 387–402, 1998.
- 857 Faegri, K. and Iversen, J.: *Textbook of Pollen Analysis*. Wiley, New York., 1989.
- 858 Fletcher, W. J. and Sánchez-Goñi, M. F.: Orbital- and sub-orbital-scale climate impacts on
859 vegetation of the western Mediterranean basin over the last 48,000 yr, *Quat. Res.*, 70(3),
860 451–464, doi:[10.1016/j.yqres.2008.07.002](https://doi.org/10.1016/j.yqres.2008.07.002), 2008.
- 861 Fletcher, W. J., Debret, M. and Sánchez-Goñi, M. F.: Mid-Holocene emergence of a low-
862 frequency millennial oscillation in western Mediterranean climate: Implications for past
863 dynamics of the North Atlantic atmospheric westerlies, *The Holocene*, 23(2), 153–166,
864 doi:[10.1177/0959683612460783](https://doi.org/10.1177/0959683612460783), 2013.
- 865 Florenzano, A., Marignani, M., Rosati, L., Fascetti, S. and Mercuri, A. M.: Are Cichorieae an
866 indicator of open habitats and pastoralism in current and past vegetation studies?, *Plant*
867 *Biosyst. - Int. J. Deal. Asp. Plant Biol.*, 149(1), 154–165,
868 doi:[10.1080/11263504.2014.998311](https://doi.org/10.1080/11263504.2014.998311), 2015.
- 869 Florschütz, F., Amor, J. M. and Wijmstra, T. A.: Palynology of a thick quaternary succession
870 in southern Spain, *Palaeogeogr. Palaeoclimatol. Palaeoecol.*, 10(4), 233–264,
871 doi:[http://dx.doi.org/10.1016/0031-0182\(71\)90049-6](http://dx.doi.org/10.1016/0031-0182(71)90049-6), 1971.
- 872 García-Alix, A., Jimenez-Espejo, F. J., Lozano, J. A., Jiménez-Moreno, G., Martínez-Ruiz,
873 F., Sanjuán, L. G., Jiménez, G. A., Alfonso, E. G., Ruiz-Puertas, G. and Anderson, R. S.:
874 Anthropogenic impact and lead pollution throughout the Holocene in Southern Iberia, *Sci.*
875 *Total Environ.*, 449, 451–460, doi:<https://doi.org/10.1016/j.scitotenv.2013.01.081>, 2013.

- 876 García-Alix, A., Jiménez-Espejo, F. J., Toney, J. L., Jiménez-Moreno, G., Ramos-Román, M.
877 J., Anderson, R. S., Ruano, P., Queralt, I., Delgado Huertas, A. and Kuroda, J.: Alpine bogs
878 of southern Spain show human-induced environmental change superimposed on long-term
879 natural variations, *Sci. Rep.*, 7(1), 7439, doi:10.1038/s41598-017-07854-w, 2017.
- 880 van Geel, B., Hallewas, D. P. and Pals, J. P.: A late holocene deposit under the Westfriesse
881 Zeedijk near Enkhuizen (Prov. of Noord-Holland, The Netherlands): Palaeoecological and
882 archaeological aspects, *Rev. Palaeobot. Palynol.*, 38(3), 269–335,
883 doi:http://dx.doi.org/10.1016/0034-6667(83)90026-X, 1983.
- 884 van Geel, B., Coope, G. R. and Hammen, T. V. D.: Palaeoecology and stratigraphy of the
885 lateglacial type section at Usselo (the Netherlands), *Rev. Palaeobot. Palynol.*, 60(1), 25–129,
886 doi:http://dx.doi.org/10.1016/0034-6667(89)90072-9, 1989.
- 887 Gil García, M. J., Ruiz Zapata, M. B., Santisteban, J. I., Mediavilla, R., López-Pamo, E. and
888 Dabrio, C. J.: Late holocene environments in Las Tablas de Daimiel (south central Iberian
889 peninsula, Spain), *Veg. Hist. Archaeobotany*, 16(4), 241–250, doi:10.1007/s00334-006-0047-
890 9, 2007.
- 891 Gil-Romera, G., Carrión, J. S., Pausas, J. G., Sevilla-Callejo, M., Lamb, H. F., Fernández, S.
892 and Burjachs, F.: Holocene fire activity and vegetation response in South-Eastern Iberia,
893 *Quat. Sci. Rev.*, 29(9), 1082–1092, doi:10.1016/j.quascirev.2010.01.006, 2010.
- 894 Grimm, E. C.: CONISS: a FORTRAN 77 program for stratigraphically constrained cluster
895 analysis by the method of incremental sum of squares, *Comput. Geosci.*, 13(1), 13–35,
896 doi:http://dx.doi.org/10.1016/0098-3004(87)90022-7, 1987.
- 897 Guy-Ohlson, D.: Botryococcus as an aid in the interpretation of palaeoenvironment and
898 depositional processes, *Rev. Palaeobot. Palynol.*, 71(1), 1–15,
899 doi:http://dx.doi.org/10.1016/0034-6667(92)90155-A, 1992.
- 900 Hurrell, J. W.: Decadal Trends in the North Atlantic Oscillation: Regional Temperatures and
901 Precipitation, *Science*, 269(5224), 676, doi:10.1126/science.269.5224.676, 1995.
- 902 Jalut, G., Dedoubat, J. J., Fontugne, M. and Otto, T.: Holocene circum-Mediterranean
903 vegetation changes: Climate forcing and human impact, *Quat. Int.*, 200(1–2), 4–18,
904 doi:https://doi.org/10.1016/j.quaint.2008.03.012, 2009.
- 905 Jiménez-Espejo, F. J., García-Alix, A., Jiménez-Moreno, G., Rodrigo-Gámiz, M., Anderson,
906 R. S., Rodríguez-Tovar, F. J., Martínez-Ruiz, F., Giralt, S., Delgado Huertas, A. and Pardo-
907 Igúzquiza, E.: Saharan aeolian input and effective humidity variations over western Europe
908 during the Holocene from a high altitude record, *Chem. Geol.*, 374–375, 1–12,
909 doi:10.1016/j.chemgeo.2014.03.001, 2014.
- 910 Jiménez-Moreno, G. and Anderson, R. S.: Holocene vegetation and climate change recorded
911 in alpine bog sediments from the Borreguiles de la Virgen, Sierra Nevada, southern Spain,
912 *Quat. Res.*, 77(1), 44–53, doi:10.1016/j.yqres.2011.09.006, 2012.
- 913 Jiménez-Moreno, G., García-Alix, A., Hernández-Corbalán, M. D., Anderson, R. S. and
914 Delgado-Huertas, A.: Vegetation, fire, climate and human disturbance history in the
915 southwestern Mediterranean area during the late Holocene, *Quat. Res.*, 79(2), 110–122,
916 doi:https://doi.org/10.1016/j.yqres.2012.11.008, 2013.

- 917 Jiménez-Moreno, G., Rodríguez-Ramírez, A., Pérez-Asensio, J. N., Carrión, J. S., López-
918 Sáez, J. A., Villarías-Robles, J. J. R., Celestino-Pérez, S., Cerrillo-Cuenca, E., León, Á. and
919 Contreras, C.: Impact of late-Holocene aridification trend, climate variability and
920 geodynamic control on the environment from a coastal area in SW Spain, *Holocene*, 25(4),
921 607–617, doi:10.1177/0959683614565955, 2015.
- 922 Kalugin, I., Daryin, A., Smolyaninova, L., Andreev, A., Diekmann, B. and Khlystov, O.:
923 800-yr-long records of annual air temperature and precipitation over southern Siberia inferred
924 from Teletskoye Lake sediments, *Quat. Res.*, 67(3), 400–410,
925 doi:https://doi.org/10.1016/j.yqres.2007.01.007, 2007.
- 926 Laskar, J., Robutel, P., Joutel, F., Gastineau, M., Correia, A. C. M. and Levrard, B.: A long-
927 term numerical solution for the insolation quantities of the Earth, *A&A*, 428(1), 261–285,
928 doi:10.1051/0004-6361:20041335, 2004.
- 929 Lebreiro, S. M., Francés, G., Abrantes, F. F. G., Diz, P., Bartels-Jónsdóttir, H. B.,
930 Stroynowski, Z. N., Gil, I. M., Pena, L. D., Rodrigues, T., Jones, P. D., Nombela, M. A.,
931 Alejo, I., Briffa, K. R., Harris, I. and Grimalt, J. O.: Climate change and coastal hydrographic
932 response along the Atlantic Iberian margin (Tagus Prodelta and Muros Ría) during the last
933 two millennia, *Holocene*, 16(7), 1003–1015, doi:10.1177/0959683606h1990rp, 2006.
- 934 Lillios, K. T., Blanco-González, A., Drake, B. L. and López-Sáez, J. A.: Mid-late Holocene
935 climate, demography, and cultural dynamics in Iberia: A multi-proxy approach, *Quat. Sci.*
936 *Rev.*, 135, 138–153, doi:https://doi.org/10.1016/j.quascirev.2016.01.011, 2016.
- 937 López-Sáez, J. A., Abel-Schaad, D., Pérez-Díaz, S., Blanco-González, A., Alba-Sánchez, F.,
938 Dorado, M., Ruiz-Zapata, B., Gil-García, M. J., Gómez-González, C. and Franco-Múgica, F.:
939 Vegetation history, climate and human impact in the Spanish Central System over the last
940 9000 years, *Quat. Int.*, 353, 98–122, doi:https://doi.org/10.1016/j.quaint.2013.06.034, 2014.
- 941 Lukianova, R. and Alekseev, G.: Long-Term Correlation Between the Nao and Solar
942 Activity, *Sol. Phys.*, 224(1), 445–454, doi:10.1007/s11207-005-4974-x, 2004.
- 943 Magny, M.: Holocene climate variability as reflected by mid-European lake-level
944 fluctuations and its probable impact on prehistoric human settlements, *Quat. Int.*, 113(1), 65–
945 79, doi:https://doi.org/10.1016/S1040-6182(03)00080-6, 2004.
- 946 Magny, M., Peyron, O., Sadori, L., Ortu, E., Zanchetta, G., Vannièrè, B. and Tinner, W.:
947 Contrasting patterns of precipitation seasonality during the Holocene in the south- and north-
948 central Mediterranean, *J. Quat. Sci.*, 27(3), 290–296, doi:10.1002/jqs.1543, 2012.
- 949 Magri, D.: Late Quaternary vegetation history at Lagaccione near Lago di Bolsena (central
950 Italy), *Rev. Palaeobot. Palynol.*, 106(3–4), 171–208, doi:https://doi.org/10.1016/S0034-
951 6667(99)00006-8, 1999.
- 952 Marchal, O., Cacho, I., Stocker, T. F., Grimalt, J. O., Calvo, E., Martrat, B., Shackleton, N.,
953 Vautravers, M., Cortijo, E., Van Kreveld, S., Andersson, C., Koç, N., Chapman, M., Saffi,
954 L., Duplessy, J.-C., Sarnthein, M., Turon, J.-L., Duprat, J. and Jansen, E.: Apparent long-term
955 cooling of the sea surface in the northeast Atlantic and Mediterranean during the Holocene,
956 *Quat. Sci. Rev.*, 21(4–6), 455–483, doi:10.1016/S0277-3791(01)00105-6, 2002.

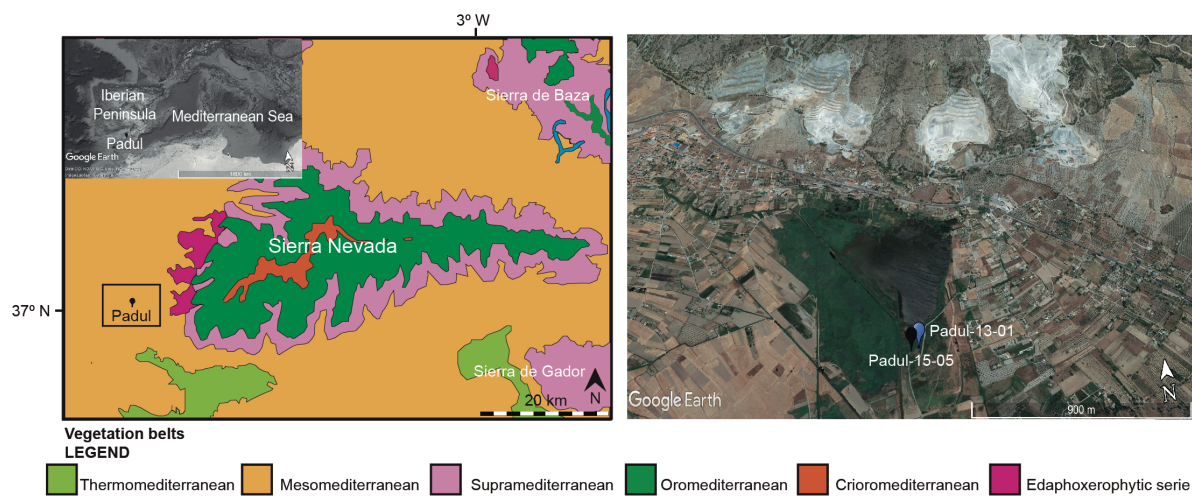
- 957 Martín-Puertas, C., Valero-Garcés, B. L., Mata, M. P., González-Sampériz, P., Bao, R.,
 958 Moreno, A. and Stefanova, V.: Arid and humid phases in southern Spain during the last 4000
 959 years: the Zoñar Lake record, Córdoba, *The Holocene*, 18(6), 907–921,
 960 doi:10.1177/0959683608093533, 2008.
- 961 Martín-Puertas, C., Valero-Garcés, B. L., Brauer, A., Mata, M. P., Delgado-Huertas, A. and
 962 Dulski, P.: The Iberian-Roman Humid Period (2600-1600 cal yr BP) in the Zoñar Lake varve
 963 record (Andalucía, southern Spain), *Quat. Res.*, 71(2), 108–120,
 964 doi:10.1016/j.yqres.2008.10.004, 2009.
- 965 Martín-Puertas, C., Valero-Garcés, B. L., Mata, M. P., Moreno, A., Giralt, S., Martínez-Ruiz,
 966 F. and Jiménez-Espejo, F.: Geochemical processes in a Mediterranean Lake: A high-
 967 resolution study of the last 4,000 years in Zoñar Lake, southern Spain, *J. Paleolimnol.*, 46(3),
 968 405–421, doi:10.1007/s10933-009-9373-0, 2011.
- 969 Mayewski, P. A., Rohling, E. E., Stager, J. C., Karlén, W., Maasch, K. A., Meeker, L. D.,
 970 Meyerson, E. A., Gasse, F., Kreveld, S. van, Holmgren, K., Lee-Thorp, J., Rosqvist, G.,
 971 Rack, F., Staubwasser, M., Schneider, R. R. and Steig, E. J.: Holocene climate variability,
 972 *Quat. Res.*, 62(3), 243–255, doi:https://doi.org/10.1016/j.yqres.2004.07.001, 2004.
- 973 Mercuri, A. M., Accorsi, C. A., Mazzanti, M. B., Bosi, G., Cardarelli, A., Labate, D.,
 974 Marchesini, M. and Grandi, G. T.: Economy and environment of Bronze Age settlements –
 975 Terramaras – on the Po Plain (Northern Italy): first results from the archaeobotanical research
 976 at the Terramara di Montale, *Veg. Hist. Archaeobotany*, 16(1), 43, doi:10.1007/s00334-006-
 977 0034-1, 2006.
- 978 Morellón, M., Valero-Garcés, B., Vegas-Vilarrúbia, T., González-Sampériz, P., Romero, Ó.,
 979 Delgado-Huertas, A., Mata, P., Moreno, A., Rico, M. and Corella, J. P.: Lateglacial and
 980 Holocene palaeohydrology in the western Mediterranean region: The Lake Estanya record
 981 (NE Spain), *Quat. Sci. Rev.*, 28(25–26), 2582–2599,
 982 doi:https://doi.org/10.1016/j.quascirev.2009.05.014, 2009.
- 983 Morellón, M., Valero-Garcés, B., González-Sampériz, P., Vegas-Vilarrúbia, T., Rubio, E.,
 984 Rieradevall, M., Delgado-Huertas, A., Mata, P., Romero, Ó., Engstrom, D. R., López-
 985 Vicente, M., Navas, A. and Soto, J.: Climate changes and human activities recorded in the
 986 sediments of Lake Estanya (NE Spain) during the Medieval Warm Period and Little Ice Age,
 987 *J. Paleolimnol.*, 46(3), 423–452, doi:10.1007/s10933-009-9346-3, 2011.
- 988 Morellón, M., Anselmetti, F. S., Ariztegui, D., Brushulli, B., Sinopoli, G., Wagner, B.,
 989 Sadori, L., Gilli, A. and Pambuku, A.: Human–climate interactions in the central
 990 Mediterranean region during the last millennia: The laminated record of Lake Butrint
 991 (Albania), *Spec. Issue Mediterr. Holocene Clim. Environ. Hum. Soc.*, 136(Supplement C),
 992 134–152, doi:10.1016/j.quascirev.2015.10.043, 2016.
- 993 Moreno, A., Cacho, I., Canals, M., Grimalt, J. O., Sánchez-Goñi, M. F., Shackleton, N. and
 994 Sierro, F. J.: Links between marine and atmospheric processes oscillating on a millennial
 995 time-scale. A multi-proxy study of the last 50,000 yr from the Alboran Sea (Western
 996 Mediterranean Sea), *Quat. Sci. Rev.*, 24(14–15), 1623–1636,
 997 doi:https://doi.org/10.1016/j.quascirev.2004.06.018, 2005.

- 998 Moreno, A., Pérez, A., Frigola, J., Nieto-Moreno, V., Rodrigo-Gámiz, M., Martrat, B.,
 999 González-Sampériz, P., Morellón, M., Martín-Puertas, C., Corella, J. P., Belmonte, Á.,
 1000 Sancho, C., Cacho, I., Herrera, G., Canals, M., Grimalt, J. O., Jiménez-Espejo, F., Martínez-
 1001 Ruiz, F., Vegas-Vilarrúbia, T. and Valero-Garcés, B. L.: The Medieval Climate Anomaly in
 1002 the Iberian Peninsula reconstructed from marine and lake records, *Quat. Sci. Rev.*, 43, 16–32,
 1003 doi:<https://doi.org/10.1016/j.quascirev.2012.04.007>, 2012.
- 1004 Nestares, T. and Torres, T. de: Un nuevo sondeo de investigación paleoambiental del
 1005 Pleistoceno y Holoceno en la turbera del Padul (Granada, Andalucía). *Geogaceta* 23, 99-102.,
 1006 1997.
- 1007 Oliva, M., Schulte, L. and Ortiz, A. G.: Morphometry and Late Holocene activity of
 1008 solifluction landforms in the Sierra Nevada, Southern Spain, *Permafr. Periglac. Process.*,
 1009 20(4), 369–382, 2009.
- 1010 Olsen, J., Anderson, N. J. and Knudsen, M. F.: Variability of the North Atlantic Oscillation
 1011 over the past 5,200 years, *Nat. Geosci.*, 5(11), 808–812, doi:10.1038/ngeo1589, 2012.
- 1012 Ortiz, J. E., Torres, T., Delgado, A., Julià, R., Lucini, M., Llamas, F. J., Reyes, E., Soler, V.
 1013 and Valle, M.: The palaeoenvironmental and palaeohydrological evolution of Padul Peat Bog
 1014 (Granada, Spain) over one million years, from elemental, isotopic and molecular organic
 1015 geochemical proxies, *Org. Geochem.*, 35(11–12), 1243–1260,
 1016 doi:<https://doi.org/10.1016/j.orggeochem.2004.05.013>, 2004.
- 1017 Paillard, D., Labeyrie, L. and Yiou, P.: Macintosh Program performs time-series analysis,
 1018 *Eos Trans. Am. Geophys. Union*, 77(39), 379–379, doi:10.1029/96EO00259, 1996.
- 1019 Pérez Raya, F. and López Nieto, J.: Vegetación acuática y helofítica de la depresión de Padul
 1020 (Granada), *Acta Bot Malacit.*, 16(2), 373–389, 1991.
- 1021 Pons, A. and Reille, M.: The holocene- and upper pleistocene pollen record from Padul
 1022 (Granada, Spain): A new study, *Palaeogeogr. Palaeoclimatol. Palaeoecol.*, 66(3), 243–263,
 1023 doi:[http://dx.doi.org/10.1016/0031-0182\(88\)90202-7](http://dx.doi.org/10.1016/0031-0182(88)90202-7), 1988.
- 1024 Ramos-Román, M. J., Jiménez-Moreno, G., Anderson, R. S., García-Alix, A., Toney, J. L.,
 1025 Jiménez-Espejo, F. J. and Carrión, J. S.: Centennial-scale vegetation and North Atlantic
 1026 Oscillation changes during the Late Holocene in the southern Iberia, *Quat. Sci. Rev.*, 143,
 1027 84–95, doi:<https://doi.org/10.1016/j.quascirev.2016.05.007>, 2016.
- 1028 Reimer, P. J., Bard, E., Bayliss, A., Beck, J. W., Blackwell, P. G., Ramsey, C. B., Buck, C.
 1029 E., Cheng, H., Edwards, R. L., Friedrich, M., Grootes, P. M., Guilderson, T. P., Haflidason,
 1030 H., Hajdas, I., Hatté, C., Heaton, T. J., Hoffmann, D. L., Hogg, A. G., Hughen, K. A., Kaiser,
 1031 K. F., Kromer, B., Manning, S. W., Niu, M., Reimer, R. W., Richards, D. A., Scott, E. M.,
 1032 Southon, J. R., Staff, R. A., Turney, C. S. M. and van der Plicht, J.: IntCal13 and Marine13
 1033 Radiocarbon Age Calibration Curves 0–50,000 Years cal BP, *Radiocarbon*, 55(4), 1869–
 1034 1887, doi:10.2458/azu_js_rc.55.16947, 2013.
- 1035 Riera, S., Wansard, G. and Julià, R.: 2000-year environmental history of a karstic lake in the
 1036 Mediterranean Pre-Pyrenees: the Estanya lakes (Spain), *{CATENA}*, 55(3), 293–324,
 1037 doi:[https://doi.org/10.1016/S0341-8162\(03\)00107-3](https://doi.org/10.1016/S0341-8162(03)00107-3), 2004.

- 1038 Riera, S., López-Sáez, J. A. and Julià, R.: Lake responses to historical land use changes in
1039 northern Spain: The contribution of non-pollen palynomorphs in a multiproxy study, *Rev.*
1040 *Palaeobot. Palynol.*, 141(1–2), 127–137, doi:<https://doi.org/10.1016/j.revpalbo.2006.03.014>,
1041 2006.
- 1042 Roberts, N., Brayshaw, D., Kuzucuoğlu, C., Perez, R. and Sadori, L.: The mid-Holocene
1043 climatic transition in the Mediterranean: Causes and consequences, *The Holocene*, 21(1), 3–
1044 13, doi:[10.1177/0959683610388058](https://doi.org/10.1177/0959683610388058), 2011.
- 1045 Rodrigo-Gámiz, M., Martínez-Ruiz, F., Rodríguez-Tovar, F. J., Jiménez-Espejo, F. J. and
1046 Pardo-Igúzquiza, E.: Millennial- to centennial-scale climate periodicities and forcing
1047 mechanisms in the westernmost Mediterranean for the past 20,000 yr, *Quat. Res.*, 81(1), 78–
1048 93, doi:<https://doi.org/10.1016/j.yqres.2013.10.009>, 2014.
- 1049 Sadori, L., Jahns, S. and Peyron, O.: Mid-Holocene vegetation history of the central
1050 Mediterranean, *The Holocene*, 21(1), 117–129, doi:[10.1177/0959683610377530](https://doi.org/10.1177/0959683610377530), 2011.
- 1051 Sadori, L., Giraudi, C., Masi, A., Magny, M., Ortu, E., Zanchetta, G. and Izdebski, A.:
1052 Climate, environment and society in southern Italy during the last 2000 years. A review of
1053 the environmental, historical and archaeological evidence, *Spec. Issue Mediterr. Holocene*
1054 *Clim. Environ. Hum. Soc.*, 136(Supplement C), 173–188,
1055 doi:[10.1016/j.quascirev.2015.09.020](https://doi.org/10.1016/j.quascirev.2015.09.020), 2016.
- 1056 Sanz de Galdeano, C., El Hamdouni, R. and Chacón, J.: Neotectónica de la fosa del Padul y
1057 del Valle de Lecrín, *Itiner. Geomorfológicos Por Andal. Orient. Publicacions Univ. Barc.*
1058 *Barc.*, 65–81, 1998.
- 1059 Sicre, M.-A., Jalali, B., Martrat, B., Schmidt, S., Bassetti, M.-A. and Kallel, N.: Sea surface
1060 temperature variability in the North Western Mediterranean Sea (Gulf of Lion) during the
1061 Common Era, *Earth Planet. Sci. Lett.*, 456, 124–133,
1062 doi:[http://dx.doi.org/10.1016/j.epsl.2016.09.032](https://doi.org/10.1016/j.epsl.2016.09.032), 2016.
- 1063 Sonett, C. P. and Suess, H. E.: Correlation of bristlecone pine ring widths with atmospheric
1064 ^{14}C variations: a climate-Sun relation, *Nature*, 307(5947), 141–143, doi:[10.1038/307141a0](https://doi.org/10.1038/307141a0),
1065 1984.
- 1066 Steinhilber, F., Beer, J. and Fröhlich, C.: Total solar irradiance during the Holocene,
1067 *Geophys. Res. Lett.*, 36(19), n/a–n/a, doi:[10.1029/2009GL040142](https://doi.org/10.1029/2009GL040142), 2009.
- 1068 Trouet, V., Esper, J., Graham, N. E., Baker, A., Scourse, J. D. and Frank, D. C.: Persistent
1069 Positive North Atlantic Oscillation Mode Dominated the Medieval Climate Anomaly,
1070 *Science*, 324(5923), 78, doi:[10.1126/science.1166349](https://doi.org/10.1126/science.1166349), 2009.
- 1071 Valle, F.: Mapa de series de vegetación de Andalucía 1: 400 000, Editorial Rueda., 2003.
- 1072 Valle Tendero, F.: Modelos de Restauración Forestal: Datos botánicos aplicados a la gestión
1073 del Medio Natural Andaluz II: Series de vegetación, Cons. Medio Ambiente Junta Andal.
1074 Sevilla, 2004.
- 1075 Villegas Molina, F.: Laguna de Padul: Evolución geológico-histórica, *Estud. Geográficos*,
1076 28(109), 561, 1967.

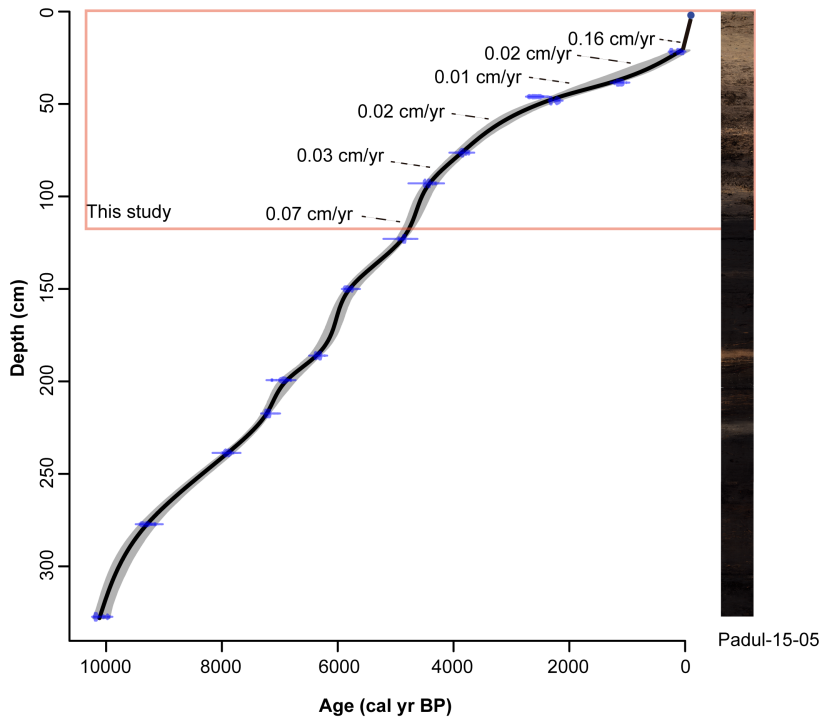
1077 Zanchettin, D., Rubino, A., Traverso, P. and Tomasino, M.: Impact of variations in solar
1078 activity on hydrological decadal patterns in northern Italy, *J. Geophys. Res. Atmospheres*,
1079 113(D12), n/a–n/a, doi:10.1029/2007JD009157, 2008.

1080 **Figures and tables**



1081

1082 **Figure 1.** Location of Padul in Sierra Nevada, southern Iberian Peninsula. Panel on the left is
1083 the map of the vegetation belts in the Sierra Nevada (Modified from REDIAM. Map of the
1084 vegetation series of Andalucía:
1085 http://laboratoriolediam.cica.es/VisorGenerico/?tipo=WMS&url=http://www.juntadeandalucia.es/medioambiente/mapwms/REDIAM_Series_Vegetacion_Andalucia?). The inset map is
1087 the Google earth image of the Iberian Peninsula in the Mediterranean region. Panel on the
1088 right is the Google earth image (<http://www.google.com/earth/index.html>) of Padul peat bog
1089 area showing the coring locations.

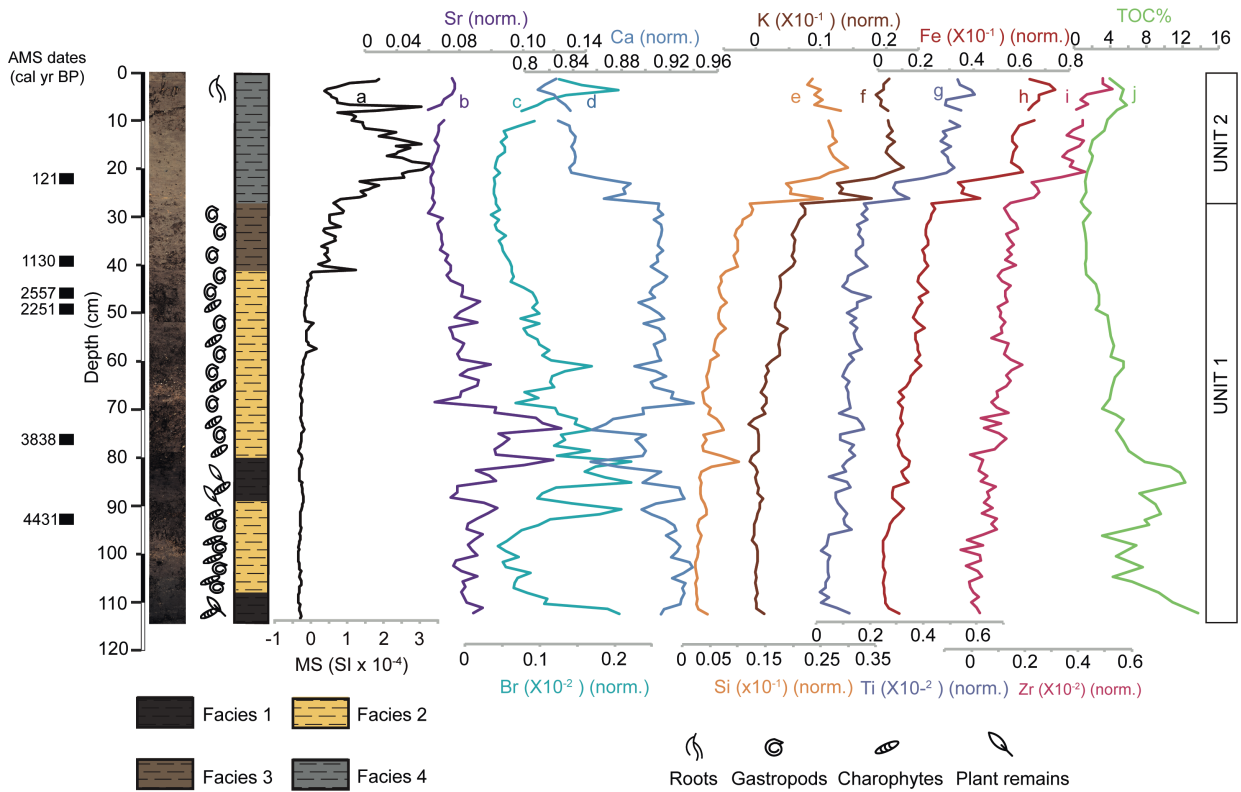


1090

1091 **Figure 2.** Photo of the Padul-15-05 sediment core with the age-depth model showing the part
 1092 of the record that was studied here (red rectangle). The sediment accumulation rates (SAR)
 1093 between individual segments are marked. See the body of the text for the explanation of the
 1094 age reconstructions.

1095

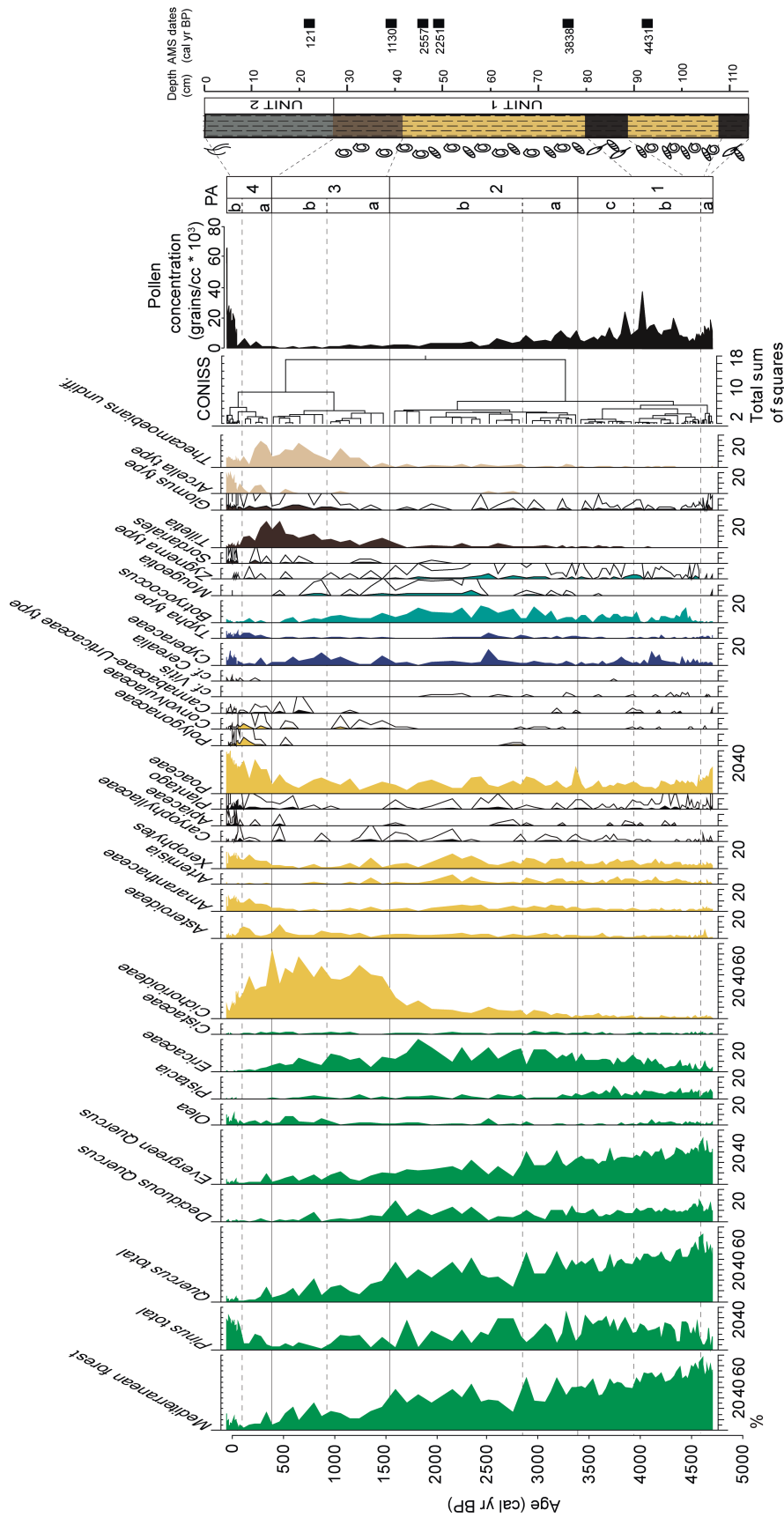
1096



1097

1098 **Figure 3.** Lithology, facies interpretation with paleontology, magnetic susceptibility (MS),
 1099 and geochemical (X-ray fluorescence (XRF) and total organic carbon (TOC) data from the
 1100 Padul-15-05 record. XRF elements are represented normalized by the total counts. (a)
 1101 Magnetic susceptibility (MS; SI units). (b) Strontium normalized (Sr; norm.). (c) Bromine
 1102 norm. (Br; norm.). (d) Calcium normalized. (Ca; norm.). (e) Silica normalized (Si; norm.). (f)
 1103 Potassium normalized (K; norm.). (g) Titanium normalized (Ti; norm.). (h) Iron normalized
 1104 (Fe; norm.). (i) Zirconium normalized (Zr; norm.). (j) Total organic carbon (TOC %). AMS
 1105 radiocarbon dates (cal yr BP) are shown on the left.

1106

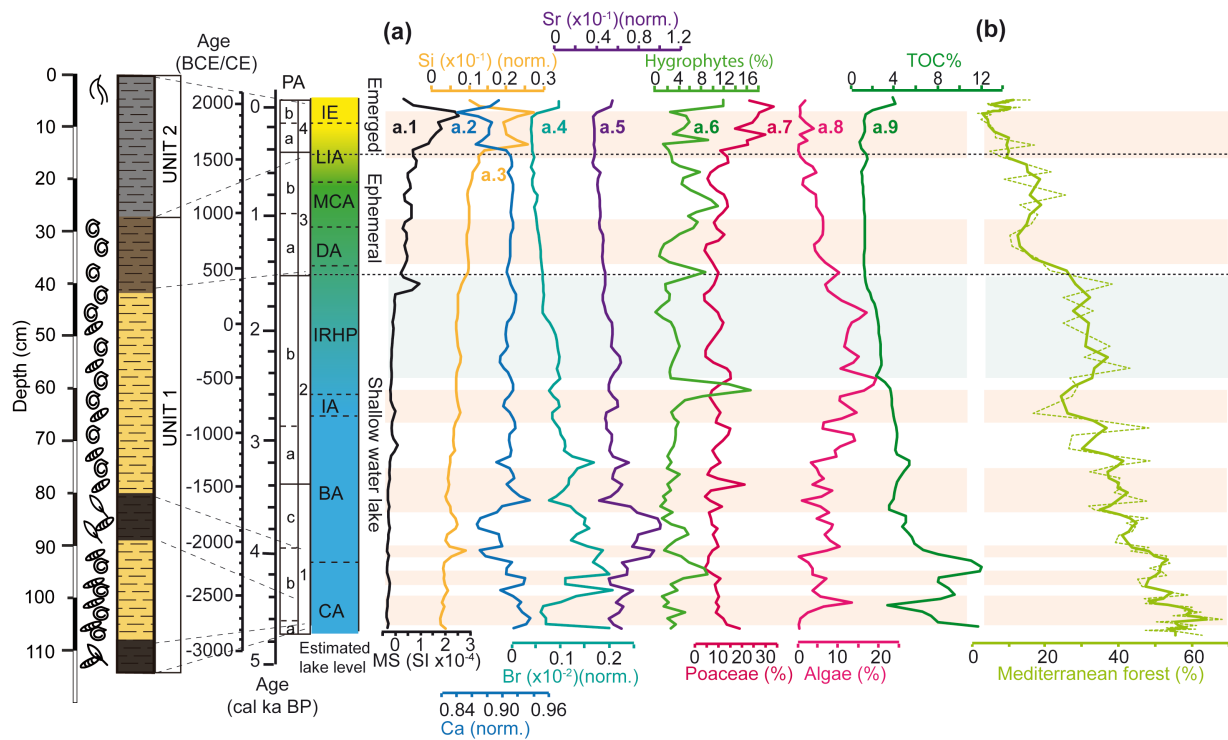


1107

1108

1109 **Figure 4.** Percentages of selected pollen taxa and non-pollen palynomorphs (NPPs) from the
1110 Padul-15-05 record, calculated with respect to terrestrial pollen sum. Silhouettes show 7-time
1111 exaggerations of pollen percentages. Pollen zonation, pollen concentration (grains/cc),
1112 lithology and AMS radiocarbon dates are shown on the right. Tree and shrubs are showing in
1113 green, herbs and grasses in yellow, aquatics in dark blue, algae in blue, fungi in brown and
1114 thecamoebians in beige. The Mediterranean forest taxa category is composed of *Quercus*
1115 total, *Olea*, *Phillyrea* and *Pistacia*. The xerophyte group includes *Artemisia*, *Ephedra*, and
1116 Amaranthaceae. PA = Pollen zones.

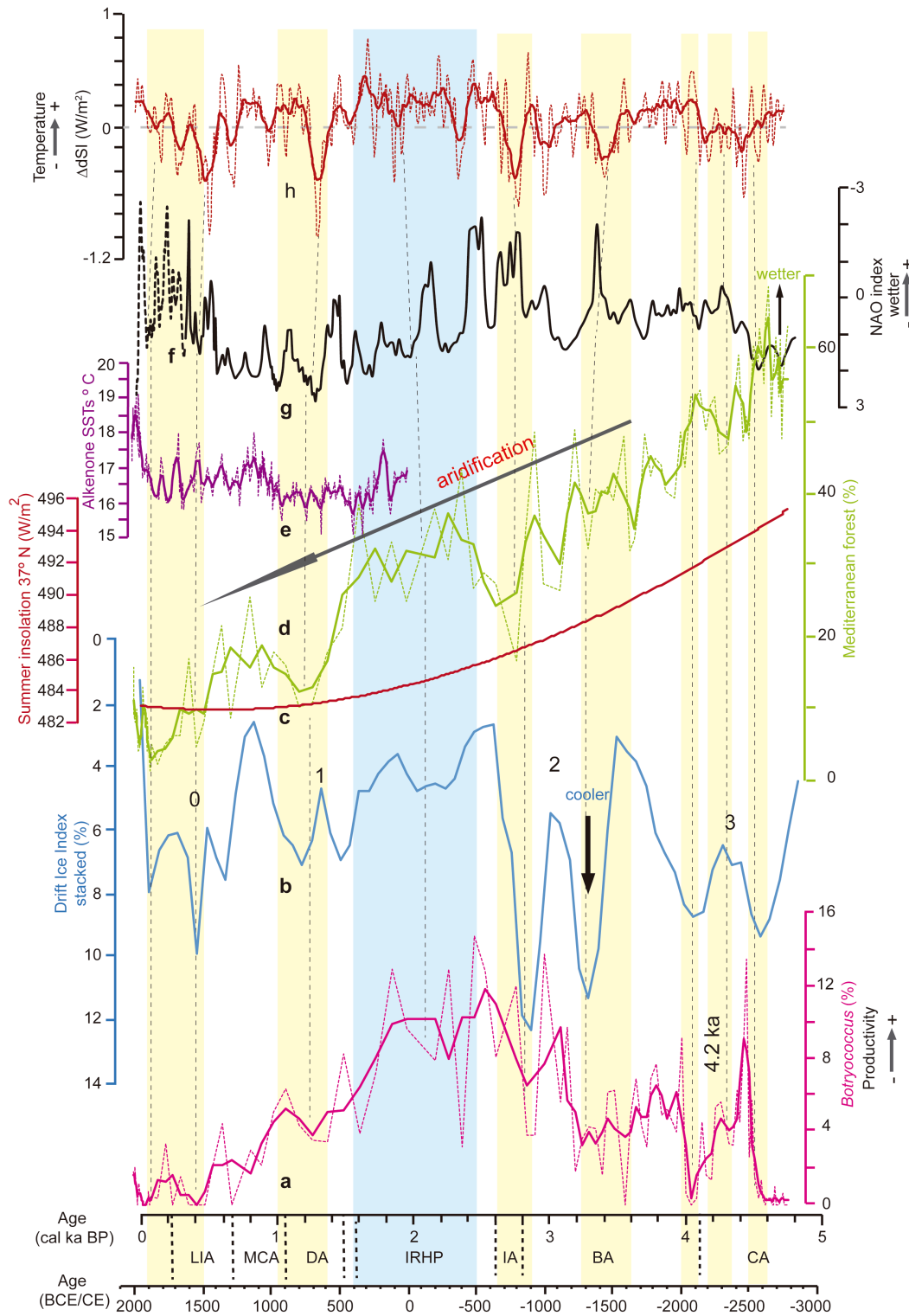
1117



1118

1119 **Figure 5.** Estimated lake level evolution and regional palynological component from the last
 1120 ca. 4700 yr based on the synthesis of determinate proxies from the Padul-15-05 record: (a)
 1121 Proxies used to estimate the water table evolution from the Padul-15-05 record (proxies were
 1122 resampled at 50 yr (lineal interpolation) using Past software [http://palaeo-
 1124 electronica.org/2001_1/past/issue1_01.htm](http://palaeo-

 1123 electronica.org/2001_1/past/issue1_01.htm)). [(a.1) Magnetic Susceptibility (MS) in SI; (a.2)
 1125 Silica normalized (Si; norm.); (a.3) Calcium normalized (Ca; norm.); (a.4) Bromine
 1126 normalized (Br; norm.); (a.5) Strontium normalized (Sr; norm.); (a.6) Hygrophytes (%); (a.7)
 1127 Poaceae (%); (a.8) Algae (%) (a.9) Total organic carbon (TOC %)] (b) Mediterranean forest
 1128 taxa, with a smoothing of three-point in bold. Pink and blue shading indicates Holocene arid
 1129 and humid regionally events, respectively. See the body of the text for the explanation of the
 1130 lake level reconstruction. Mediterranean forest smoothing was made using Analyseries
 1131 software (Paillard et al., 1996). PA = Pollen Zones; CA = Copper Age; BA = Bronze Age; IA
 1132 = Iron Age; IRHP = Iberian Roman Humid Period; DA = Dark Ages; MCA = Medieval
 Climate Anomaly; LIA = Little Ice Age; IE = Industrial Era.



1133

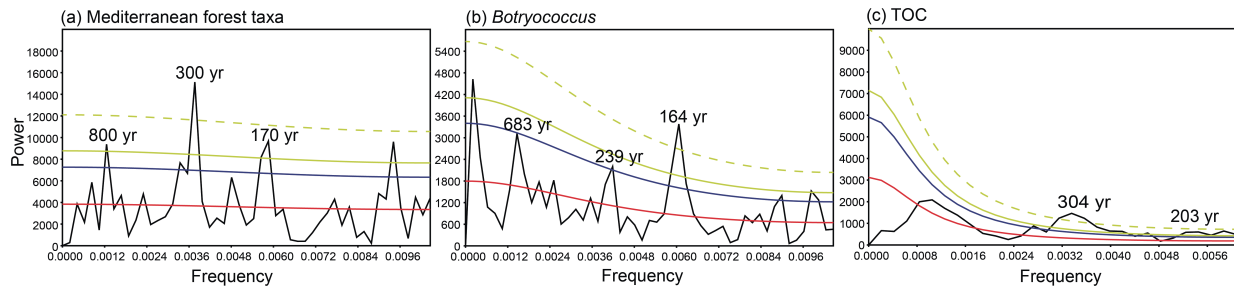
1134

1135 **Figure 6.** Comparison of the last ca. 4700 yr between different pollen taxa from the Padul-
 1136 15-05 record, summer insolation for the Sierra Nevada latitude, eastern Mediterranean
 1137 humidity and North Atlantic temperature. (a) *Botryococcus* from the Padul-15-05 record,
 1138 with a smoothing of three-point in bold (this study). (b) Drift Ice Index (reversed) from the
 1139 North Atlantic (Bond et al., 2001). (c) Summer insolation calculated for 37° N (Laskar et al.,
 1140 2004). (d) Mediterranean forest taxa from the Padul-15-05 record, with a smoothing of three-

1141 point in bold (this study). (e) Alkenone-SSTs from the Gulf of Lion (Sicre et al., 2016), with
1142 a smoothing of four-point in bold. (f) North Atlantic Oscillation (NAO) index from a climate
1143 proxy reconstruction from Morocco and Scotland (Trouet et al., 2009). (g) North Atlantic
1144 Oscillation (NAO) index (reversed) from a climate proxy reconstruction from Greenland
1145 (Olsen et al., 2012). (h) Total solar irradiance reconstruction from cosmogenic radionuclide
1146 from a Greenland ice core (Steinhilber et al., 2009), with a smoothing of twenty-one-point in
1147 bold. Note that the magnitude of the different curves is not in the same scale. Yellow and
1148 blue shading correspond with arid (and cold) and humid (and warm) periods, respectively.
1149 Grey dash lines show a tentative correlation between arid and cold conditions and the
1150 decrease in the Mediterranean forest and *Botryococcus*. Mediterranean forest, *Botryococcus*
1151 and solar irradiance smoothing was made using Analyseries software (Paillard et al., 1996),
1152 Alkenone-SSTs smoothing was made using Past software ([http://palaeo-](http://palaeo-electronica.org/2001_1/past/issue1_01.htm)
1153 [electronica.org/2001_1/past/issue1_01.htm](http://palaeo-electronica.org/2001_1/past/issue1_01.htm)). A linear r (Pearson) correlation was calculated
1154 between *Botryococcus* (detrended) and Drift Ice Index (Bond et al., 2001; $r = -0.63$; $p <$
1155 0.0001 ; between ca. 4700 to 1500 cal ka BP – $r = -0.48$; $p < 0.0001$ between 4700 and -65 cal
1156 yr BP). Previously, the data were detrended (only in *Botryococcus*), resampled at 70-yr
1157 (linear interpolation) in order to obtain equally spaced time series and smoothed to three-
1158 point average. CA = Copper Age; BA = Bronze Age; IA = Iron Age; IRHP = Iberian Roman
1159 Humid Period; DA = Dark Ages; MCA = Medieval Climate Anomaly; LIA = Little Ice Age;
1160 IE = Industrial Era.

1161

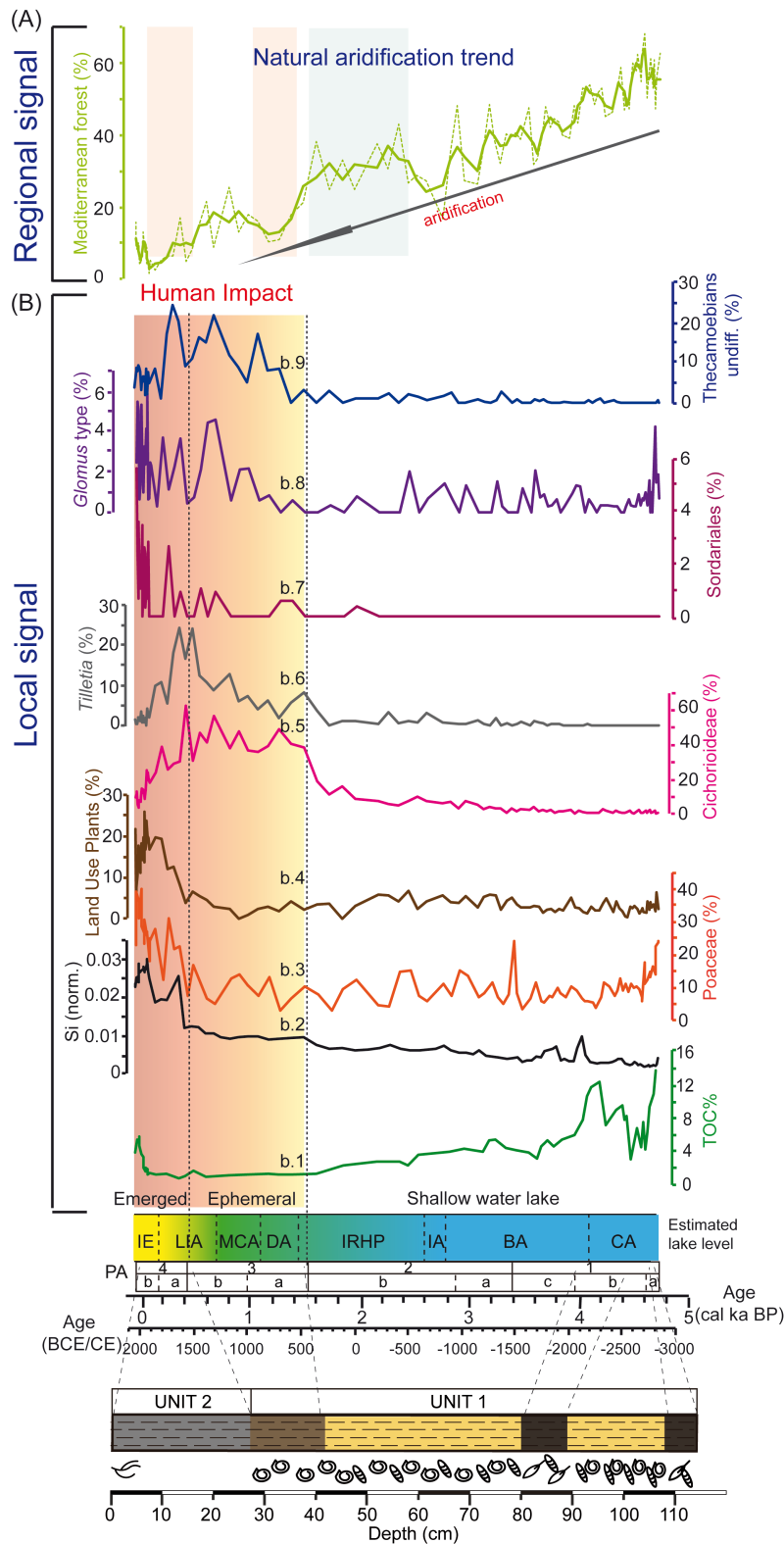
1162



1163

1164 **Figure 7.** Spectral analysis of (a) Mediterranean forest taxa and (b) *Botryococcus* (mean
 1165 sampling space = 47 yr) and (c) TOC (mean sampling space = 78 yr) from the Padul-15-05.
 1166 The significant periodicities above confident level are shown. Confidence level 90 % (blue
 1167 line), 95 % (green line), 99 % (green dash line) and AR (1) red noise (red line). Spectral
 1168 analysis was made with Past software ([http://palaeo-](http://palaeo-electronica.org/2001_1/past/issue1_01.htm)
 1169 [electronica.org/2001_1/past/issue1_01.htm](http://palaeo-electronica.org/2001_1/past/issue1_01.htm)).

1170



1171

1172 **Figure 8.** Comparison of the last ca. 4700 yr between regional climatic proxies and local
 1173 human activity indicators from the Padul-15-05 record. (A) Mediterranean forest taxa, with a
 1174 smoothing of three-point in bold. (B) Local human activities indicators [(b.1) Total organic
 1175 carbon (TOC %), soil erosion indicator; (b.2) Si normalized (Si, norm.), soil erosion
 1176 indicator; (b.3) Poaceae (%), lake drained and/or cultivars indicator; (b.4) Land Use Plants
 1177 (%), cultivar indicator; (b.5) Cichorioideae (%), livestock occurrence indicator; (b.6) *Tilletia*

1178 (%), farming indicator; (b.7) Sordariales (%), livestock indicator; (b.8) *Glomus* type, soil
1179 erosion, (b.9) Thecamoebians undiff. (%), livestock indicator]. Degraded yellow to red
1180 shading correspond with the time when we have evidence of human shaping the environment
1181 since ca. 1550 cal yr BP to Present. Previously to that period there is a lack of clear evidences
1182 of human impact in the area. Land use plants is composed by Polygonaceae, Amaranthaceae,
1183 Convolvulaceae, *Plantago*, Apiaceae and Cannabaceae-Urticaceae type.

1184 **Table 1.** Age data for Padul-15-05 record. All ages were calibrated using R-code package
 1185 ‘clam 2.2’ employing the calibration curve IntelCal 13 (Reimer et al., 2013) at 95 % of
 1186 confident range.

1187 *Sample number assigned at radiocarbon laboratory

Laboratory number	Core	Material	Depth (cm)	Age (^{14}C yr BP $\pm 1\sigma$)	Calibrated age (cal yr BP) 95 % confidence interval	Median age (cal yr BP)
Reference ages			0	2015CE	-65	-65
D-AMS 008531	Padul-13-01	Plant remains	21.67	103 \pm 24	23-264	127
Poz-77568	Padul-15-05	Org. bulk sed.	38.46	1205 \pm 30	1014-1239	1130
BETA-437233	Padul-15-05	Plant remains	46.04	2480 \pm 30	2385-2722	2577
Poz-77569	Padul-15-05	Org. bulk sed.	48.21	2255 \pm 30	2158-2344	2251
BETA-415830	Padul-15-05	Shell	71.36	3910 \pm 30	4248-4421	4343
BETA- 437234	Padul-15-05	Plant remains	76.34	3550 \pm 30	3722-3956	3838
BETA-415831	Padul-15-05	Org. bulk sed.	92.94	3960 \pm 30	4297-4519	4431
Poz-74344	Padul-15-05	Plant remains	122.96	4295 \pm 35	4827-4959	4871
BETA-415832	Padul-15-05	Plant remains	150.04	5050 \pm 30	5728-5900	5814
Poz-77571	Padul-15-05	Plant remains	186.08	5530 \pm 40	6281-6402	6341
Poz-74345	Padul-15-05	Plant remains	199.33	6080 \pm 40	6797-7154	6935
BETA-415833	Padul-15-05	Org. bulk sed.	217.36	6270 \pm 30	7162-7262	7212
Poz-77572	Padul-15-05	Org. bulk sed.	238.68	7080 \pm 50	7797-7999	7910
Poz-74347	Padul-15-05	Plant remains	277.24	8290 \pm 40	9138-9426	9293
BETA-415834	Padul-15-05	Plant remains	327.29	8960 \pm 30	9932-10221	10107

1188

1189

1190 **Table 2.** Linear r (Pearson) correlation between geochemical elements from the Padul-15-05
 1191 record. Statistical treatment was performed using the Past software ([http://palaeo-
 electronica.org/2001_1/past/issue1_01.htm](http://palaeo-

 1192 electronica.org/2001_1/past/issue1_01.htm)).

1193

	Si	K	Ca	Ti	Fe	Zr	Br	Sr
Si		8.30E-80	2.87E-34	7.47E-60	3.22E-60	5.29E-44	0.001152	7.79E-09
K	0.98612		7.07E-29	6.05E-60	8.20E-68	1.77E-51	0.00030317	5.38E-12
Ca	-0.88096	-0.84453		6.09E-42	5.81E-39	8.10E-34	0.35819	0.26613
Ti	0.96486	0.96501	-0.91794		1.74E-74	1.12E-57	0.074223	8.88E-07
Fe	0.96546	0.97577	-0.90527	0.98224		2.77E-66	0.051072	3.32E-08
Zr	0.92566	0.94789	-0.8783	0.96109	0.97398		0.054274	7.16E-08
Br	-0.31739	-0.3506	-0.091917	-0.17755	-0.19372	-0.19116		4.03E-18
Sr	-0.53347	-0.61629	0.11113	-0.46426	-0.51386	-0.50295	0.72852	

1194

1195

1196

1197

1198

1199

1200

1201

1202

1203

1204

1205

1206

1207

1208

1209